Three-dimensional finite element computations for frictional contact problems with non-associated sliding rule

Mohammed Hjiaj, Zhi-Qiang Feng, Géry de Saxcé, Zenon Mróz

Three-dimensional finite element computations for frictional contact problems with non-associated sliding rule

M. Hjiaj[1,*,†], Z-Q Feng[2], G. de Saxcé[3] and Z. Mróz[4]

1School of Engineering, The University of Newcastle, University Drive, Callaghan NSW 2308, Australia
2Université d'Évry Val d'Essonne, Laboratoire de Mécanique d'Évry (LME), EA 3332 40,
rue du Pelvoux 91020 Évry cédex, France
3Laboratoire de Mécanique de Lille UMR CNRS 8107, Boulevard Paul Langevin, Cité Scientifique, 59655
Villeneuve d'Ascq cédex, France
4Institute of Fundamental Technological Research, Polish Academy of Sciences, ´Swi¸etokrzyska 21,
PL 00-049, Warsaw, Poland

This paper presents an algorithm for solving anisotropic frictional contact problems where the sliding rule is non-associated. The algorithm is based on a variational formulation of the complex interface model that combine the classical unilateral contact law and an anisotropic friction model with a non-associated slip rule. Both the friction condition and the sliding potential are elliptical and have the same principal axes but with different semi-axes ratio. The frictional contact law and its inverse are derived from a single non-differentiable scalar-valued function, called a bi-potential. The convexity properties of the bi-potential permit to associate stationary principles with initial/boundary value problems. With the present formulation, the time-integration of the frictional contact law takes the form of a projection onto a convex set and only one predictor–corrector step addresses all cases (sticking, sliding, no-contact). A solution algorithm is presented and tested on a simple example that shows the strong influence of the slip rule on the frictional behaviour.

KEY WORDS: anisotropic friction condition; non-associated sliding rule; variational formulation; bi-potential; time stepping; augmented Lagrangian technique

1. INTRODUCTION

Contact problems involving friction are of crucial importance in many engineering branches. When bodies come into contact, and friction exists on the contact surface, in addition to normal forces, friction (shear) forces appear on the contact plane that resist sliding. The frictional

*Correspondence to: Mohammed Hjiaj, School of Engineering, The University of Newcastle, University Drive, Callaghan NSW 2308, Australia.
†E-mail:mohammed.hjiaj@newcastle.edu.au

Contract/grant sponsor: Publishing Arts Research Council; contract/grant number: 98-1846389

behaviour on the contact surface is often assumed to be independent of the sliding velocity (rate-independent frictional law). In engineering applications such as wear, lubrication and rolling, a precise description of the frictional behaviour on the contact surface is required. This has stimulated the development of mathematical models of friction that need to be implemented in numerical tools (FEM). The interface law describing the interactions between bodies on the contact surface, called frictional contact law, is built up from two different mechanisms: contact and friction.

The unilateral contact law involves two conditions [1]. The first one is impenetrability, which specify that a body must not cross the boundary of the other body when they come into contact, i.e. the distance between the two bodies is non-negative. The second condition is non-adhesion that is the normal component of the reaction force is non-negative (compression). Frictional effects are generally accounted for by the introduction of a frictional law that relates the friction force and the corresponding tangential relative velocity. It has partly a static character in that it specifies a set of admissible contact forces (friction condition), and partly an evolutional character in that it specifies what directions of sliding are allowed (sliding rule). If the later aspect is introduced into a problem one has to view all variables as time dependant. The friction condition specifies that friction forces can be exerted without sliding, i.e. under stick conditions, until a certain threshold is overcome to allow sliding. In Coulomb's law, the threshold is proportional to the contact pressure and when sliding occurs, the frictional forces always oppose the sliding velocity and are, therefore, dissipative.

The friction condition is generally assumed to be isotropic, that is the frictional behaviour is independent of the sliding direction. For many industrial applications, this assumption seems to be unrealistic and the frictional behaviour can change drastically with the sliding direction, requiring an anisotropic model. The origin of anisotropy can be attributed to two different sources. The first one is the material itself. The anisotropies of the materials constituting the bodies manifest themselves on the contact surface as well. The second one is technological; the industrial process used to fabricate the bodies can create striations along preferential directions. In fact, most machining, finishing and superfinishing operations are directional, and machined surfaces have particular striation patterns unique to a type of machining. For a large number of machining processes, the striation directions are mutually orthogonal. For such surfaces, an orthotropic friction condition will provide a better description of the frictional behaviour.

In papers devoted to orthotropic frictional contact problems, an associated sliding rule in the contact plane is assumed, although there is no particular reason for preventing the sliding rule being non-associated. Furthermore, experimental evidence shows that the sliding rule can deviate significantly from the normal to the friction condition in the plane $r_n = \text{const}$, where r_n is the contact pressure (normal component of the stress vector). This fact was pointed out by Michałowski and Mróz [2]. By considering a model of rigid anisotropic asperities, they have shown that, in general, a non-associated sliding rule occurs within the contact plane with a possible concavity of the limit friction surface. In contrast, the classical isotropic Coulomb's law preserves the normality of slips to the friction cone (which is convex) in this plane.

The non-associativity within the friction force plane for a specified contact pressure undoubtedly complicates the numerical solution of boundary value problems involving such non-standard frictional contact models. Indeed, problems implicating the simple ideal friction model with an associated sliding rule are considered among the most difficult in solid mechanics. The source of mathematical and numerical difficulties is the lack of a pseudo-potential such that

its subgradients yield back the frictional contact law. The inexistence of a pseudo-potential is a straightforward consequence of the non-associated character of the frictional contact law. In fact, if we regard force and velocity as conjugate quantities of each other, the normality will not occur since it would require that the velocity would have a normal separating component. On the other hand, if we consider admissible to include a dependence of the pseudo-potential on the state, the normality holds and we have a family of pseudo-potentials. In this way it is possible to treat, within the concept of a Generalized Standard Material [3–5], phenomena such as friction with a constant normal force and non-associated plasticity models where the normality rule is satisfied in the deviatoric plane. This state-dependant pseudo-potential is called *quasi-pseudo-potential*. The term 'quasi' is used to emphasize its dependence on the state. The existence of a quasi-pseudo-potential results from the partly associated character of the law. These ideas have been exploited by Alart and Curnier [6] in the derivation of their popular algorithm for frictional contact problems.

An alternative way to the state-dependant pseudo-potential is the *bi-potential*. In this formalism, introduced by de Saxcé and Feng [7], the evolution law along with its inverse are derived from a single bi-convex function called a bi-potential. The advantage of this formalism is that the normality, essential for stationary (or extremum) principles, is conserved, but in an implicit form. The approach has been applied successfully to several non-standard models [8, 9]. An outcome of the approach is a robust time-integration of the frictional contact law and the existence of coupled stationary principles. By adopting the same formalism, we extend the previous work on isotropic Coulomb's frictional contact law to anisotropic friction conditions with non-associated sliding rule. It has been shown that, general friction contact law with anisotropic friction condition and non-associated sliding rule can be derived from a bi-potential [10]. Here, a numerical algorithm based on this variational formulation is presented. The present work is a continuation and an extension of previous work carried out by de Saxcé and Feng [7, 11]. The numerical example treated shows the applicability and the robustness of the method.

The aim of this paper is to present a unified algorithm for the solution of initial/boundary value problems involving anisotropic interface models with a non-associated sliding rule. For reasons, which will appear clear later, the present study is restricted to convex friction conditions. In the next section, some basic definitions are recalled and notations specified. The unilateral contact law is recalled. In particular, when bodies are already in contact, the impenetrability condition can be written either in terms of displacements or velocities. Section 3 is concerned with an anisotropic friction model with a convex limit friction surface and a non-associated sliding rule. At the end of this section, the rate form of the Signorini conditions is coupled with the sliding rule to give the complete frictional contact law for contacting bodies. In Section 4, classical variational formulations of the contact law and the slip rule are discussed in depth. Next, details concerning the derivation of the bi-potential are given. It is shown that the frictional contact law along with its inverse can be derived from this single scalar-valued function. In Section 5, continuous and discretized forms of the evolution problem associated with the frictional contact phenomenon are addressed. Section 6 deals with the governing discrete relations of the considered frictional contact model. In Section 7, the discretized frictional contact problem is outlined and the F.E. algorithm is presented in Section 8. The example shown in Section 9 demonstrates the robustness of the algorithm. It can be seen that the slip rule (associated or non-associated) has a significant effect on the frictional behaviour.

2. SETTING OF THE PROBLEM

In the following, basic definitions and notations used are described. Symmetric second-order tensor are represented by six-dimensional vectors. Bold letters are used for vectors and 'T' in exponent stands for the usual transposition. As discussed in the introduction, the problem under consideration is evolutionary. Therefore, all variables need to be viewed as time dependent. However, since the problem is rate independent, the parameter t measures the order of events rather than the physical time. So, the study is performed during a time interval, which corresponds to the loading process assumed to be quasistatic and isothermal.

Two deformable bodies $\mathscr{B}^\alpha$ (Figure 1), $\alpha = 1, 2$, are considered. Each of them occupies the open, simply connected, bounded domain $\Omega^\alpha \subset \mathbb{R}^3$, whose generic point is denoted $\mathbf{X}^\alpha$. Furthermore, the solids are elastic and undergo small deformations. The boundary Γ^α of each body is assumed to be sufficiently smooth everywhere such that an outward unit normal vector, denoted by $\mathbf{n}^\alpha$, can be defined at any point M on Γ^α. At each time $t \in \mathbf{I}$, where $\mathbf{I} = [0, T]$ denotes the time interval corresponding to the loading process, the boundary Γ^α of the body $\mathscr{B}^\alpha$ can, in general, be split into three parts: Γ_u^α with prescribed displacements $\bar{\mathbf{u}}^\alpha$, Γ_t^α with prescribed boundary loads $\bar{\mathbf{t}}^\alpha$, and the potential contact surfaces Γ_c^α where the two bodies $\mathscr{B}^1$ and $\mathscr{B}^2$ may possibly come into contact at some time t:

$$\Gamma^\alpha = \Gamma_u^\alpha \cup \Gamma_t^\alpha \cup \Gamma_c^\alpha \tag{1}$$

Each body $\mathscr{B}^\alpha$ satisfy, at each time t, the local equilibrium equations

$$\operatorname{div} \boldsymbol{\sigma}^\alpha + \bar{\mathbf{f}}^\alpha = \mathbf{0} \quad \text{in } \Omega^\alpha \tag{2}$$

$$\mathbf{n}^\alpha \boldsymbol{\alpha}^\alpha = \bar{\mathbf{t}}^\alpha \quad \text{on } \Gamma_t^\alpha \tag{3}$$

where $\boldsymbol{\sigma}$ is the Cauchy stress tensor and $\bar{\mathbf{f}}^\alpha$ are prescribed body forces. The successive deformed configurations of $\mathscr{B}^\alpha$ are described at each time t by the displacement fields $\mathbf{u}^\alpha$ defined on $\bar{\Omega}^\alpha$ (i.e. the closure of Ω^α), which satisfy the compatibility requirements

$$\boldsymbol{\varepsilon}^\alpha = \operatorname{grad}_s \mathbf{u}^\alpha \quad \text{in } \Omega^\alpha \tag{4}$$

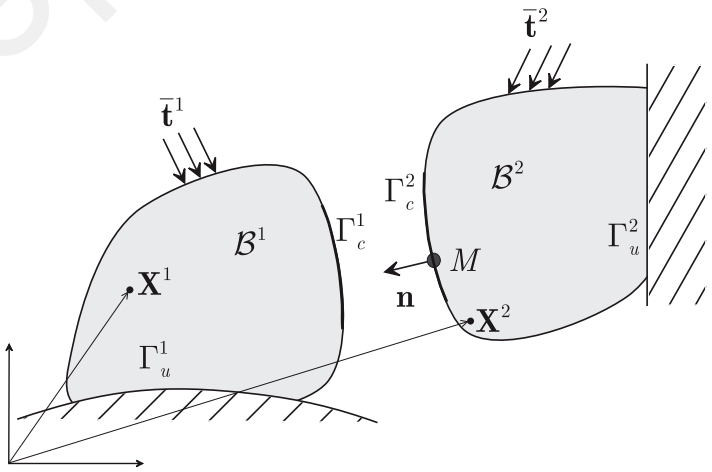

Figure 1. Contact mechanics.

$$\mathbf{u}^\alpha = \bar{\mathbf{u}}^\alpha \quad \text{on } \Gamma_u^\alpha \tag{5}$$

where $\boldsymbol{\varepsilon}$ is the strain tensor and grad_s the symmetric part of the gradient. The bodies $\mathscr{B}^\alpha$ are assumed to be linear elastic. The stress-strain relationship derives from a convex quadratic elastic energy potential $V(\boldsymbol{\varepsilon}^\alpha)$

$$\boldsymbol{\sigma}^\alpha = \frac{\partial V(\boldsymbol{\varepsilon}^\alpha)}{\partial \boldsymbol{\varepsilon}^\alpha} \tag{6}$$

The potential $V(\boldsymbol{\varepsilon}^\alpha)$ and its complementary $W(\boldsymbol{\sigma}^\alpha)$ satisfy the following inequality:

$$V(\boldsymbol{\varepsilon}^\alpha) + W(\boldsymbol{\sigma}^\alpha) \geqslant \boldsymbol{\varepsilon}^\alpha \cdot \boldsymbol{\sigma}^\alpha \tag{7}$$

which becomes a strict equality for pairs $(\boldsymbol{\sigma}^\alpha, \boldsymbol{\varepsilon}^\alpha)$ related by the constitutive law. On the contact surface, a unique normal $\mathbf{n}$ directed towards $\mathscr{B}^1$ ($\mathbf{n} \equiv \mathbf{n}^2$) is defined and the tangential plane, orthogonal to $\mathbf{n}$ in $\mathbb{R}^3$, is denoted by $\mathbf{T}$. To construct an orthonormal local basis, two unit vectors $\mathbf{t}_x$ and $\mathbf{t}_y$ are defined within the plane $\mathbf{T}$. For describing the frictional contact interactions that may occur on Γ_c, we introduce the relative velocity with respect to $\mathscr{B}^2$

$$\dot{\mathbf{u}} = \dot{\mathbf{u}}^1 - \dot{\mathbf{u}}^2 \tag{8}$$

where $\dot{\mathbf{u}}^1$ and $\dot{\mathbf{u}}^2$ are the instantaneous velocities of $\mathscr{B}^1$ and $\mathscr{B}^2$, respectively. Let $\mathbf{r}$ be the contact force distribution exerted on $\mathscr{B}^1$ at M from $\mathscr{B}^2$. According to the action-reaction principle, $\mathscr{B}^2$ is subjected to the stress vector $-\mathbf{r}$. In the local coordinate system defined by the tangential plane $\mathbf{T}$ and the normal $\mathbf{n}$, any element $\dot{\mathbf{u}}$ and $\mathbf{r}$ may be uniquely decomposed as

$$\dot{\mathbf{u}} = \dot{\mathbf{u}}_t + \dot{u}_n \mathbf{n}, \quad \dot{\mathbf{u}}_t \in \mathbf{T}, \quad \dot{u}_n \in \mathbb{R} \tag{9}$$

$$\mathbf{r} = \mathbf{r}_t + r_n \mathbf{n}, \quad \mathbf{r}_t \in \mathbf{T}, \quad r_n \in \mathbb{R} \tag{10}$$

The unilateral contact law is characterized by a geometric condition of non-penetration, a static condition of no-adhesion and a mechanical complementary condition. These three conditions are known as the Signorini conditions. The non-penetration condition constraints the displacement fields $\mathbf{u}^\alpha$ and is given by

$$g(\mathbf{X}^1) = (\mathbf{X}^1 - \mathbf{X}^2) \cdot \mathbf{n} \geqslant 0 \tag{11}$$

where

$$\mathbf{X}^\alpha(t) = \mathbf{X}^\alpha(t = 0) + \mathbf{u} \tag{12}$$

The position vector $\mathbf{X}^2$ is found as the closest-point projection of the point $\mathbf{X}^1 \in \Gamma_c^1$ on the surface Γ_c^2. Denoting by h the initial gap

$$h = (\mathbf{X}^1(t = 0) - \mathbf{X}^2(t = 0)) \cdot \mathbf{n} \geqslant 0$$

the Signorini conditions are given by

$$u_n + h \geqslant 0, \quad r_n \geqslant 0, \quad (u_n + h) r_n = 0 \tag{13}$$

These conditions have to be satisfied at each time-instant $t \in \mathbf{I}$. Assume now that the bodies are initially in contact on a certain portion of Γ_c. On this part of Γ_c, the Signorini conditions turns into

$$u_n \geqslant 0, \quad r_n \geqslant 0, \quad u_n r_n = 0 \tag{14}$$

In general, at any time $t \in \mathbf{I}$, the potential contact surfaces Γ_c^α can be split into two disjoint parts: ${}^+\Gamma_c$ where the bodies are already in contact and ${}^-\Gamma_c^\alpha$ where the body are not in contact:

$$\Gamma_c^\alpha = {}^+\Gamma_c \cup {}^-\Gamma_c^\alpha \tag{15}$$

In contrast to Γ_c^α, ${}^+\Gamma_c$ and ${}^-\Gamma_c^\alpha$ change in time t and can be empty at some $t \in \mathbf{I}$. We must stress that with the formulation (14) only a loss of contact is allowed and the extension of the contact area cannot be modeled with these relations. On ${}^+\Gamma_c$, the Signorini conditions can be formulated in terms of relative velocity

$$\dot{u}_n \geqslant 0, \quad r_n \geqslant 0, \quad \dot{u}_n r_n = 0 \quad \text{on } {}^+\Gamma_c \tag{16}$$

When $\dot{u}_n \geqslant 0$, the bodies are separating while they remain in contact for $\dot{u}_n = 0$. The previous formulation of the Signorini conditions (16) can be combined with the sliding rule to derive the complete frictional contact law applicable on the contacting part of Γ_c. This complete law specifies possible velocities of bodies that satisfy impenetrability, non-adhesion and the sliding rule. Obviously, for a strictly positive gap ($u_n \geqslant 0$), the normal relative velocity is arbitrary ($\dot{u}_n \in \mathbb{R}$) and the normal reaction force is equal to zero ($r_n = 0$). Motions of bodies that are not in contact are arbitrary until contact is made. This choice is motivated by the fact that the emphasis is put on the definition of admissible evolutions for contacting bodies where the time-integration has to be performed. In the rest of the paper, a sign 'minus' will always precede the relative tangential velocity $-\dot{\mathbf{u}}_t$ to emphasize its opposite direction to the friction force.

3. GENERAL ANISOTROPIC MODELS WITH NON-ASSOCIATED SLIDING RULE

As a rule, a velocity-independent friction model is assumed, as well as a linear dependence of the limit tangential force on the normal force. This model corresponds to a Coulomb-type frictional behaviour. By considering a model of asperity interaction, a family of friction conditions and sliding rules was derived by Michałowski and Mróz [2] (see also Reference [12]). They concluded that the level curves of the sliding potential can be approximated by ellipses and the friction condition can have an arbitrary form, not necessarily convex. Therefore, the sliding rule is no longer associated with the limit friction condition in the plane $r_n = \text{const}$ as it occurs when the sliding potential coincides (up to an arbitrary constant) with the friction condition for a known contact pressure. In this paper, non-convex sliding potentials are excluded and only anisotropic friction models, described by a friction condition and a sliding potential of elliptical form (in the plane $r_n = \text{const}$) are considered. The principal axes of both ellipses coincide with the orthogonal orthotropy axes x and y. A non-associated sliding rule is then

obtained by simply choosing different principal semi-axes ratios for the friction criterion and the sliding potential. Such models, although simple, provide a valuable insight into the character of limit friction and sliding rules.

3.1. Anisotropic friction condition

The asperity model used by Michałowski and Mróz [2] to study anisotropic frictional contact phenomenon generates limit friction curves in the contact plane that can be slightly non-convex but very close to ellipses. Here, we consider only convex friction conditions that have the following form:

$$f(r_{t_x}, r_{t_y}, r_n) = \|\mathbf{r}_t\|_\mu - r_n = 0 \tag{17}$$

where $\| \bullet \|_\mu$ denotes the elliptic norm

$$\|\mathbf{r}_t\|_\mu = \sqrt{\left(\frac{r_{t_x}}{\mu_x}\right)^2 + \left(\frac{r_{t_y}}{\mu_y}\right)^2} = \|\mathbb{M}^{-1}\mathbf{r}_t\| \tag{18}$$

with

$$\mathbb{M} = \begin{bmatrix} \mu_x & 0 \\ 0 & \mu_y \end{bmatrix} \tag{19}$$

Ellipse (17) intersects the x-axis at $\mu_x r_n$ and $-\mu_x r_n$; it intersects the y-axis at $\mu_y r_n$ and $-\mu_y r_n$ where the coefficients μ_x and μ_y are the principal friction coefficients. The classical isotropic Coulomb's friction condition is recovered by setting

$$\mu_x = \mu_y = \mu \tag{20}$$

The set of admissible forces, denoted K_μ and defined by

$$K_\mu = \{\mathbf{r} \in \mathbb{R}^3 \mid \|\mathbf{r}_t\|_\mu - r_n \leqslant 0\} \tag{21}$$

is convex. The dual norm $\| \bullet \|_\mu^*$ associated to (18) is given by

$$\| -\dot{\mathbf{u}}_t\|_\mu^* = \sqrt{\mu_x^2(-\dot{u}_{t_x})^2 + \mu_y^2(-\dot{u}_{t_y})^2} = \|\mathbb{M}(-\dot{\mathbf{u}}_t)\|_\mu^* \tag{22}$$

3.2. Rate form of the sliding rule

The convex slip potential has also elliptical level curves but with different semi-axes ratio (Figure 2) and is defined by

$$g(r_{t_x}, r_{t_y}) = \|\mathbf{r}_t\|_p - a = 0 \tag{23}$$

in which $\|\mathbf{r}_t\|_p$ is given by

$$\|\mathbf{r}_t\|_p = \sqrt{\left(\frac{r_{t_x}}{p_x}\right)^2 + \left(\frac{r_{t_y}}{p_y}\right)^2} = \|\mathbb{P}^{-1}\mathbf{r}_t\| \tag{24}$$

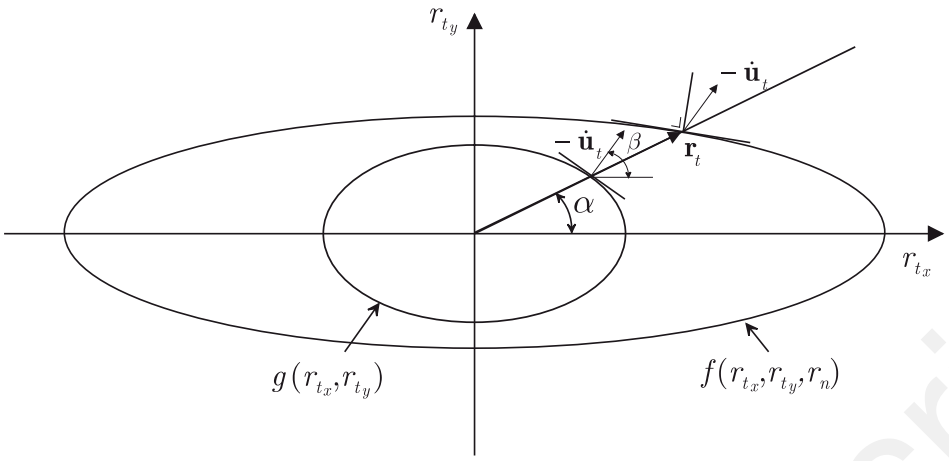

Figure 2. Friction condition and sliding rule.

with

$$\mathbb{P} = \begin{bmatrix} p_x & 0 \\ 0 & p_y \end{bmatrix} \tag{25}$$

and a is a constant whose magnitude is irrelevant. The semi-axes ratio of the slip potential is related to that of the friction condition by the following relation:

$$\frac{p_y}{p_x} = \left(\frac{\mu_y}{\mu_x}\right)^k \tag{26}$$

In the general case, we have $k \neq 1$, which leads to a non-associated sliding rule

$$-\dot{u}_n = 0 \tag{27}$$

$$-\dot{u}_{t_x} = \dot{\lambda}\frac{\partial g}{\partial r_{t_x}} = \dot{\lambda}\,\frac{r_{t_x}}{p_x^2\,\|\mathbf{r}_t\|_p} \tag{28}$$

$$-\dot{u}_{t_y} = \dot{\lambda}\frac{\partial g}{\partial r_{t_y}} = \dot{\lambda}\,\frac{r_{t_y}}{p_y^2\,\|\mathbf{r}_t\|_p} \tag{29}$$

where the multiplier $\dot{\lambda}$ is equal to

$$\dot{\lambda} = \|-\dot{\mathbf{u}}_t\|_p^* = \sqrt{p_x^2(-\dot{u}_{t_x})^2 + p_y^2(-\dot{u}_{t_y})^2} \tag{30}$$

Equivalently, the sliding rule can be written as

$$-\dot{u}_{t_x} = \dot{\lambda}'\,\frac{r_{t_x}}{p_x^2\|\mathbf{r}_t\|_\mu}, \quad -\dot{u}_{t_y} = \dot{\lambda}'\,\frac{r_{t_y}}{p_y^2\|\mathbf{r}_t\|_\mu} \tag{31}$$

In this case, the multiplier $\dot{\lambda}'$ is equal to

$$\dot{\lambda}' = \|\mathbb{Q}(-\dot{\mathbf{u}}_t)\|_p^* \tag{32}$$

where

$$\mathbb{Q} = \mathbb{P}\mathbb{M}^{-1} = \mathbb{M}^{-1}\mathbb{P} = \begin{bmatrix} \dfrac{p_x}{\mu_x} & 0 \\ 0 & \dfrac{p_y}{\mu_y} \end{bmatrix} \tag{33}$$

is called the *sliding non-associativity* matrix. Obviously, relations exist between different norms. For example, it holds

$$\|\mathbb{Q}(-\dot{\mathbf{u}}_t)\|_p^* = \|\mathbb{Q}^2(-\dot{\mathbf{u}}_t)\|_\mu^* \tag{34}$$

The dissipation function is given by

$$\mathscr{D} = r_{t_x}(-\dot{u}_{t_x}) + r_{t_y}(-\dot{u}_{t_y}) = \|\mathbf{r}_t\|_p \, \|(-\dot{\mathbf{u}}_t)\|_p^* \tag{35}$$

Using the relations between different norms, different but equivalent expressions of the dissipation function can be derived. For an associated sliding rule, we recover the classical dependence of the dissipation on the normal pressure:

$$\mathscr{D} = r_n \|(-\dot{\mathbf{u}}_t)\|_\mu^* \tag{36}$$

During sliding, the $\mathbf{r}(-\dot{\mathbf{u}})$ relationship is given by

$$r_n > 0 \tag{37}$$

$$r_{t_x} = r_n \, \frac{p_x^2(-\dot{u}_{t_x})}{\|\mathbb{Q}(-\dot{\mathbf{u}}_t)\|_p} \tag{38}$$

$$r_{t_y} = r_n \, \frac{p_y^2(-\dot{u}_{t_y})}{\|\mathbb{Q}(-\dot{\mathbf{u}}_t)\|_p} \tag{39}$$

Denoting the inclination of the shear stress vector $\mathbf{r}_t$ to the x-axis by α and that of the tangential velocity vector $(-\dot{\mathbf{u}}_t)$ by β (see Figure 2), it follows from (38) and (39) that

$$\tan\beta = \left(\frac{p_x}{p_y}\right)^2 \tan\alpha \tag{40}$$

3.3. Complete frictional contact law

We consider now the previous friction law embedding an impenetrability condition for completeness. On the contact surface ${}^{+}\Gamma_c$, the sliding rule can be combined with the rate form of the Signorini conditions to obtain the frictional contact law that specifies possible scenarios on the contact area (stick, slip, separation). The multivalued nature of this strongly non-linear law makes problems involving frictional contact among the most difficult ones in solid mechanics. The complete form of the frictional contact law involves three possible states, which are separating, contact with sticking, and contact with sliding. Only the last state produces dissipation.

Two overlapped '*if...then...else*' statements can be used to write it analytically:

$$
\begin{array}{l}
\textit{if } r_n = 0 \textit{ then} \\
\quad \dot{u}_n \geqslant 0 \qquad\qquad\qquad\qquad\qquad\qquad\qquad\qquad\qquad \text{! separating} \\
\textit{elseif } \mathbf{r} \in \operatorname{int} K_\mu \textit{ then} \\
\quad \dot{u}_n = 0 \text{ and } \dot{\mathbf{u}}_t = \mathbf{0} \qquad\qquad\qquad\qquad\qquad\qquad\qquad \text{! sticking} \\
\textit{else } (\mathbf{r} \in \operatorname{bd} K_\mu \text{ and } r_n > 0) \\
\quad \left\{ \dot{u}_n \geqslant 0 \text{ and } \exists\ \dot{\lambda} \text{ such that } -\dot{\mathbf{u}}_t = \dot{\lambda} \dfrac{\mathbb{P}^{-2}\,\mathbf{r}_t}{\|\mathbf{r}_t\|_p} \right\} \qquad \text{! sliding} \\
\textit{endif}
\end{array}
\tag{41}
$$

where '$\operatorname{int} K_\mu$' and '$\operatorname{bd} K_\mu$' denote the interior and the boundary of K_μ, respectively. The multivalued character of the law lies in the first and the second part of the statement. If r_n is null then is arbitrary but its normal component $\dot{u}_n$ should be positive. In others words, one single element of $\mathbb{R}^3$ ($\mathbf{r} = \mathbf{0}$) is associated with an infinite number of velocity vectors $\dot{\mathbf{u}} \in \mathbb{R}^3$. Same arguments can be developed for the second part of the statement. The inverse law, i.e. the relationship $\mathbf{r}(-\dot{\mathbf{u}})$, can be written as

$$
\begin{array}{l}
\textit{if } \dot{u}_n > 0 \textit{ then} \\
\quad r_n = 0 \qquad\qquad\qquad\qquad\qquad\qquad\qquad\qquad\qquad \text{! separating} \\
\textit{elseif } \dot{\mathbf{u}} = \mathbf{0} \textit{ then} \\
\quad \mathbf{r} \in K_\mu \qquad\qquad\qquad\qquad\qquad\qquad\qquad\qquad\qquad \text{! sticking} \\
\textit{else } (\dot{\mathbf{u}} \in \mathbf{T} - \{\mathbf{0}\}) \\
\quad \left\{ \dot{u}_n \geqslant 0 \text{ and } \mathbf{r}_t = r_n \dfrac{\mathbb{P}^2(-\dot{\mathbf{u}}_t)}{\|\mathbb{Q}(-\dot{\mathbf{u}}_t)\|_p^*} \right\} \qquad \text{! sliding} \\
\textit{endif}
\end{array}
\tag{42}
$$

4. VARIATIONAL FORM OF THE FRICTIONAL CONTACT LAW

The previous forms of the frictional contact law are not very enlightening as no particular mathematical structure can be recognized. With the numerical solution of boundary value problems in mind, it is of interest to briefly discuss alternative formulations of the interface law (41). Before addressing the complete frictional contact law, classical variational formulations of the unilateral contact law and the associated sliding rule are recalled. Next, the contact law is combined with the sliding rule in a single variational inequality, which suggests a particular scalar-valued function called a bi-potential. It is shown that the frictional contact law (41) and its inverse (42) can be derived from the bi-potential using a normality rule. This section ends by deriving the bi-potential expression for the non-associated sliding rule.

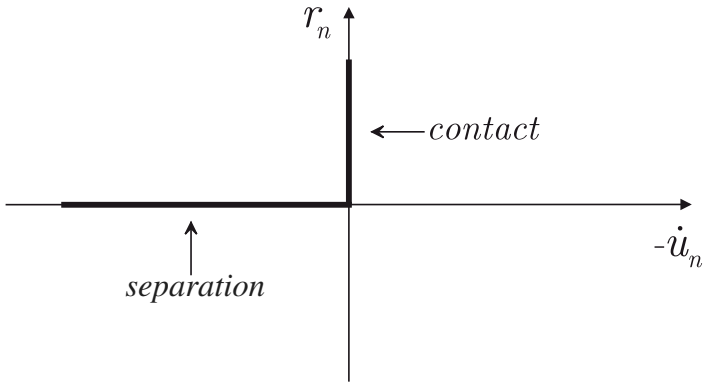

Figure 3. Unilateral contact law.

4.1. Variational formulations of the Signorini conditions

The graph of the unilateral contact law, shown on Figure 3, is not a graph of a mapping in the classical sense. Indeed, neither $-\dot{u}_n$ is a function of r_n nor r_n is a function of $-\dot{u}_n$. This is a typical example of a non-smooth relation. There is an infinite number of straight lines with positive slope in contact with the graph at $-\dot{u}_n = 0$. Accordingly, classical tools of differential calculus are not longer applicable but Convex Analysis provides an appropriate framework to deal with such graph. With the help of basic mathematical manipulations, it is possible to transform (16) into the following variational inequality:

$$r_n \in \mathbb{R}_+ : \ -\dot{u}_n(r_n - r_n') \geqslant 0, \quad \forall r_n' \in \mathbb{R}_+ \tag{43}$$

Although the previous formulation bears some nice properties, it can be further rearranged to obtain the (set-valued) constitutive mapping relating the normal velocity $-\dot{u}_n$ and the corresponding contact pressure r_n, i.e. the relation $-\dot{u}_n(r_n)$. The idea, due to Moreau [13, 14], is to make use of the indicator function [15] of the set to which the contact pressures r_n and r_n' are required to belong, i.e. $\mathbb{R}_+ = [0, +\infty[$:

$$\Psi_{\mathbb{R}_+}(r_n) = \begin{cases} 0 & \text{if } r_n \in \mathbb{R}_+ \\ +\infty & \text{otherwise} \end{cases} \tag{44}$$

This function is not differentiable in the classical sense. However the indicator function is convex if the set to which it refers is convex. Having at hand this tool, a key-step is to rewrite the variational inequality (43) in the following manner:

$$-\dot{u}_n(r_n - r_n') + \Psi_{\mathbb{R}_+}(r_n') \geqslant \Psi_{\mathbb{R}_+}(r_n) \tag{45}$$

where the member function '$\in$' in (43) has been replaced by the value of the indicator function at the corresponding contact pressure. The inequality (45) corresponds to the *convexity inequality* applied to a non-differentiable function [15]. It means that $-\dot{u}_n$ belongs to the subdifferential of $\Psi_{\mathbb{R}_+}$ at r_n or equivalently, $-\dot{u}_n$ and r_n are related by the differential inclusion:

$$-\dot{u}_n \in \partial\Psi_{\mathbb{R}_+}(r_n) \tag{46}$$

The subdifferential of $\Psi_{\mathbb{R}_+}$ at r_n corresponds to the set of all subgradients of $\Psi_{\mathbb{R}_+}$ at r_n and defines a multivalued mapping from $\mathbb{R}$ into itself:

$$\partial\Psi_{\mathbb{R}_+} : \mathbb{R} \mapsto \mathbb{R} : r_n \mapsto \partial\Psi_{\mathbb{R}_+}(r_n) \tag{47}$$

In particular, for a differentiable function, the subdifferential is reduced to a singleton which corresponds to the classical gradient. The function $\Psi_{\mathbb{R}_+}(r_n)$ is called complementary contact pseudo-potential and denoted by $\psi_C^*(r_n)$. The term 'pseudo' is used to make a distinction between the classical differentiable potential like the one existing in Hookean elasticity and the present non-differentiable potential. The above considerations show that by simply allowing the potential to be non-differentiable, a 'potential structure' of the relationship between $-\dot{u}_n$ and r_n can be produced. Accordingly, differentiable potentials are suited only for single-valued law and non-differentiable potentials provide an effective means to represent multivalued constitutive laws. With setting (46), the relationship may be inverted by applying the Fenchel transform

$$\psi_C(-\dot{u}_n) = \sup_{r_n}[-\dot{u}_n r_n - \psi_C^*(r_n)] = \Psi_{\mathbb{R}_-}(-\dot{u}_n) \tag{48}$$

where $\mathbb{R}_-$ corresponds to $]-\infty, 0]$ and ψ_C is the contact pseudo-potential. The inverse contact law is then

$$r_n \in \partial\psi_C(-\dot{u}_n) \tag{49}$$

which is equivalent to

$$r_n((-\dot{u}_n) - (-\dot{u}_n')) + \Psi_{\mathbb{R}_-}(-\dot{u}_n') \geqslant \Psi_{\mathbb{R}_-}(-\dot{u}_n) \tag{50}$$

It results from the previous inequality that

$$(-\dot{u}_n) \in \mathbb{R}_- : \quad r_n((-\dot{u}_n) - (-\dot{u}_n')) \geqslant 0, \quad \forall(-\dot{u}_n') \in \mathbb{R}_- \tag{51}$$

which is the dual of (43). The formulations (46) and (49) of the unilateral contact law are particularly useful for associating dual extremum principles to boundary value problems involving frictionless contact.

4.2. Variational formulations of the sliding rule

The graph of 2D Coulomb's law is displayed Figure 4. This graph is 'infinitely steep' and for that reason it can not be the graph of a single-valued mapping. Because r_n may take any arbitrary positive value, the graph should be considered as a family of monotone multivalued mappings.

As a first step, an associated sliding rule in the contact plane is assumed. By 'freezing' the normal reaction r_n, the friction condition (17) becomes a function of the friction force $\mathbf{r}_t$ only, and the slip law can be expressed under the form of a quasi-variational inequality:

$$\mathbf{r}_t \in \tilde{K}_\mu : (-\dot{\mathbf{u}}_t) \cdot (\mathbf{r}_t - \mathbf{r}_t') \geqslant 0, \quad \forall \mathbf{r}_t' \in \tilde{K}_\mu \tag{52}$$

where $\tilde{K}_\mu$ defined by

$$\tilde{K}_\mu = \{\mathbf{r}_t \in \mathbb{R}^2 \mid \|\mathbf{r}_t\|_\mu \leqslant k\} \quad \text{with } k = r_n \tag{53}$$

is the section of Coulomb's cone at level r_n. The term 'quasi' is used to emphasize the dependence of $\tilde{K}_\mu$ on r_n. The previous inequality suggests that the friction law can be formulated

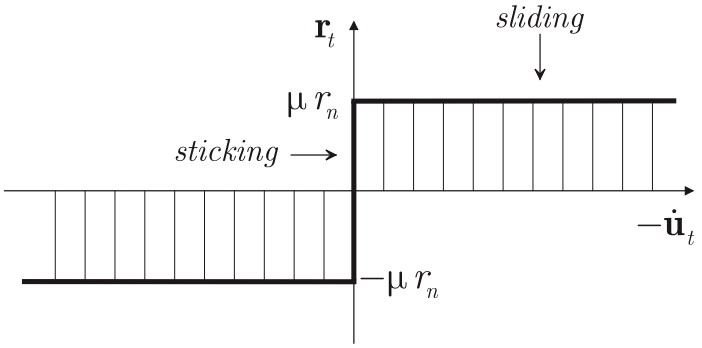

Figure 4. Coulomb's friction law.

in the form of the *principle of maximum dissipation*: the actual friction force is an optimal solution for the maximization problem in the variable $\mathbf{r}_t$:

$$\begin{aligned} &\text{maximize } (-\dot{\mathbf{u}}_t)\cdot\mathbf{r}_t \\ &\text{subject to } \mathbf{r}_t \in \tilde{K}_\mu \end{aligned} \tag{54}$$

To further transform inequality (52) in the same way it has been done for the unilateral contact law, we introduce the indicator function of the closed convex set $\tilde{K}_\mu$ defined by

$$\Psi_{\tilde{K}_\mu}(\mathbf{r}_t) = \begin{cases} 0 & \text{if } \mathbf{r}_t \in \tilde{K}_\mu \\ +\infty & \text{otherwise} \end{cases} \tag{55}$$

This function is subsequently used to enforce the constraints on the friction force:

$$(-\dot{\mathbf{u}}_t)\cdot(\mathbf{r}'_t - \mathbf{r}_t) + \Psi_{\tilde{K}_\mu}(\mathbf{r}'_t) \geqslant \Psi_{\tilde{K}_\mu}(\mathbf{r}_t) \tag{56}$$

Inequality (56) corresponds to convexity condition applied to $\Psi_{\tilde{K}_\mu}$. Therefore, it means that $(-\dot{\mathbf{u}}_t)$ belongs to the subdifferential of $\Psi_{\tilde{K}_\mu}(\mathbf{r}_t)$:

$$-\dot{\mathbf{u}}_t \in \partial\Psi_{\tilde{K}_\mu}(\mathbf{r}_t) \tag{57}$$

The indicator function $\Psi_{\tilde{K}_\mu}$ corresponds to the complementary frictional dissipation function, denoted by ψ_F^*. Because of its dependence on r_n, ψ_F^* is a quasi-pseudo-potential. Again, $\partial\Psi_{\tilde{K}_\mu}(\mathbf{r}_t)$ is a set-valued mapping and the relation (57) coincide with the sliding rule. Applying the Fenchel transform

$$\psi_F(-\dot{\mathbf{u}}_t) = \sup_{\mathbf{r}_t}\left[(-\dot{\mathbf{u}}_t)\cdot\mathbf{r}_t - \Psi_{\tilde{K}_\mu}(\mathbf{r}_t)\right] = \sup_{\mathbf{r}_t\in\tilde{K}_\mu}\left[(-\dot{\mathbf{u}}_t)\cdot\mathbf{r}_t\right] \tag{58}$$

the inversion of the slip rule is achieved

$$\mathbf{r}_t \in \partial\psi_F(-\dot{\mathbf{u}}_t) \tag{59}$$

where $\psi_F(-\dot{\mathbf{u}}_t)$ is the so-called *quasi-pseudo-potential of dissipation*. The quasi-pseudo-potential is a convex (by construction) and a positively homogenous function of order one with respect

to $-\dot{\mathbf{u}}_t$ [16]. It does not exist if the sliding rule is non-associated. The two quasi-pseudo-potentials are related by the Fenchel inequality

$$\psi_F(-\dot{\mathbf{u}}_t') + \psi_F^*(\mathbf{r}_t') \geqslant (-\dot{\mathbf{u}}_t') \cdot \mathbf{r}_t' \quad \forall (-\dot{\mathbf{u}}_t', \mathbf{r}_t') \in \mathbb{R}^3 \times \mathbb{R}^3 \tag{60}$$

The equality is reached for a pair $(-\dot{\mathbf{u}}_t, \mathbf{r}_t)$ satisfying the sliding rule

$$\psi_F(-\dot{\mathbf{u}}_t) + \psi_F^*(\mathbf{r}_t) = (-\dot{\mathbf{u}}_t) \cdot \mathbf{r}_t \tag{61}$$

The work of Moreau [13] on the mathematical structure of mechanical laws is an important step in material modeling. The main contribution is probably the unified framework proposed for mechanical laws including the multi-valued ones. The chief idea is to consider non-differentiable potential if the constitutive relation is multi-valued. To properly deal with such functions, Moreau used concepts and tools of Convex Analysis. Particularly, the notion of indicator function has been proved fruitful to the treatment of rate-independent model. The corresponding formulation and its variational structure revealed by the 'potential form' of the constitutive relationship prove to be useful regarding to the numerical and mathematical aspects of boundary value problems. This property ensures the existence of stationary principles that becomes minimum principles if the functional is convex. We recall that the existence of a potential is independent of the question of convexity [17]. We can say on one hand that a single-valued law can be derived from a differentiable potential if it exists. On the other hand, a multivalued law can be derived from a non-differentiable potential under the assumption that it exists. The non-differentiability precisely reflects the multivalued character of the physical law. Another key-step has been accomplished by Nguyen Quoc Son [3–5, 19] who extended Moreau's work to more complex multivalued laws ('visco'-plasticity with hardening, damage,...) using the phenomenological approach with internal variables. Although the introduction of the pseudo-potential concept is an important step in the formulation of the behaviour of materials, some models do not fit into this framework. Probably, the frictional contact law is the most familiar one among such models.

4.3. Variational formulation of the frictional contact law

The separate description of contact and friction in the previous sections should not hide the strong coupling existing between the two phenomena since in Coulomb's law the friction force is proportional to the contact pressure. The difficulty is that this coupling is not symmetric since the contact pressure is independent of the friction force. This results in the non-existence of a genuine frictional dissipation pseudo-potential. The frictional contact law (for bodies in contact) can be constructed by combining the contact law (46) and the sliding rule (57). This formulation was used by Alart and Curnier [6] and successfully exploited to derive a robust algorithm, which remains very competitive when compared to other more recent algorithms [18]. However, this formulation involves two scalar-valued functions and exists only if the sliding rule is associated in the plane $r_n = \text{const}$. In what follows, a general formulation of frictional contact laws with non-associated sliding rule based on a single variational inequality is presented. As a result, a relationship between $\mathbf{r}$ and $-\dot{\mathbf{u}}$ based on the normality can be recovered but only in a implicit form. For the sake of clarity, we present in details the formulation for the isotropic friction law with an associated sliding rule. At the end of this section, the result is given for the anisotropic friction condition with a non-associated slip rule.

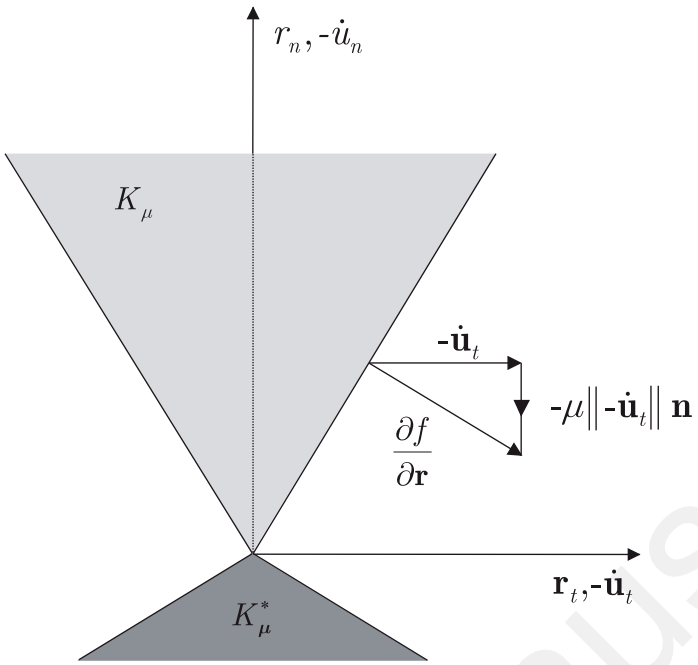

Figure 5. Non-normality of the velocity vector.

4.3.1. Associated sliding rule. It has been pointed out by many authors that friction law bears some resemblance with the flow rule in plasticity. This analogy can be further extended to the frictional contact law for bodies in contact. Let us examine Figure 5 (isotropic friction criterion) and assume that the sliding rule is associated. For the sliding status, the normality rule can be recovered by adding '$\mu\| - \dot{\mathbf{u}}_t\|\mathbf{n}$' to Coulomb's cone normal:

$$-\dot{\mathbf{u}}_t \in \partial\Psi_{K_\mu}(\mathbf{r}) + \mu\| - \dot{\mathbf{u}}_t\|\mathbf{n} \tag{62}$$

where K_μ is the isotropic Coulomb's cone:

$$K_\mu = \{\mathbf{r} \in \mathbb{R}^3 \mid \|\mathbf{r}_t\| \leqslant \mu\, r_n\} \tag{63}$$

Since the friction cone is differentiable everywhere except at the origin ($r_n = 0$), the previous relation is equivalent to

$$-\dot{\mathbf{u}}_t = \dot{\lambda}\frac{\partial f}{\partial \mathbf{r}} + \mu\| - \dot{\mathbf{u}}_t\|\mathbf{n} \tag{64}$$

for a non-null contact pressure. Since during sliding $\dot{u}_n$ is equal to zero, we can add $\dot{u}_n$ to the last term

$$-\dot{\mathbf{u}}_t = \dot{\lambda}\frac{\partial f}{\partial \mathbf{r}} + (\dot{u}_n + \mu\| - \dot{\mathbf{u}}_t\|)\mathbf{n} \tag{65}$$

without violating the sliding rule. By rearranging (65), we find that the sliding rule takes the following form:

$$-(\dot{\mathbf{u}}_t + (\dot{u}_n + \mu\| - \dot{\mathbf{u}}_t\|)\mathbf{n}) \in \partial\Psi_{K_\mu}(\mathbf{r}) \tag{66}$$

The developments leading to relation (66) are possible because the friction condition is convex explaining why we have restricted our study to such friction criterion. The construction detailed above can be viewed as a mapping $\mathscr{T}$ from $\mathbb{R}^3$ into itself:

$$\mathscr{T} : \mathbb{R}^3 \mapsto \mathbb{R}^3 : -\dot{\mathbf{u}} \mapsto -(\dot{\mathbf{u}}_t + (\dot{u}_n + \|(-\dot{\mathbf{u}}_t)\|)\mathbf{n}) \tag{67}$$

For the sake of clarity, let us denotes the transformed velocity vector by $\mathbf{v}$

$$\mathbf{v} := \mathscr{T}(-\dot{\mathbf{u}}) \tag{68}$$

and writes the frictional contact law (66) as

$$\mathbf{v} \in \partial \Psi_{K_\mu}(\mathbf{r}) \tag{69}$$

This differential inclusion is equivalent to the convexity inequality

$$\mathbf{v} \cdot (\mathbf{r}' - \mathbf{r}) + \Psi_{K_\mu}(\mathbf{r}') \geqslant \Psi_{K_\mu}(\mathbf{r}) \tag{70}$$

which can be rewritten as

$$\mathbf{r} \in K_\mu : \quad \mathbf{v} \cdot (\mathbf{r} - \mathbf{r}') \geqslant 0, \quad \forall \mathbf{r}' \in K_\mu \tag{71}$$

Relation (71) has been derived under the assumption of sliding and we need to show that this relation is also valid for the sticking and the separating cases. For $\mathbf{r}$ belonging to the interior of K_μ, it is easy to see that inequality (71) is satisfied only if the vector $\mathbf{v}$ is null. It is well known from Convex Analysis [15] that the normal cone to a convex set is the null vector for elements belonging to its interior. Decomposition (9) being unique, the condition $\mathbf{v} = \mathbf{0}$ implied that

$$\mathbf{v}_t := -\dot{\mathbf{u}}_t = \mathbf{0} \quad \text{and} \quad v_n = -(\dot{u}_n + \|(-\dot{\mathbf{u}}_t)\|) = 0 \tag{72}$$

Therefore $\dot{\mathbf{u}}$ vanishes and the corresponding status is sticking. As a last step, we need to prove that the relation (69) addresses the separating case. At this point $\mathbf{r} = \mathbf{0}$, the subdifferential of Ψ_{K_μ} coincides with the dual cone K_μ^*

$$\partial \Psi_{K_\mu}(\mathbf{0}) = K_\mu^* \tag{73}$$

defined by

$$K_\mu^* = \left\{ \mathbf{v} \in \mathbb{R}^3 \mid \mu \|\mathbf{v}_t\| + v_n \leqslant 0 \right\} \tag{74}$$

As a consequence of the duality between the cones, we have at $\mathbf{v} = \mathbf{0}$,

$$\partial \Psi_{K_\mu^*}(\mathbf{0}) = K_\mu \tag{75}$$

It is easy to show that if $\mathbf{r} = \mathbf{0}$, the condition $\mathbf{v} \in K_\mu^*$ corresponds to the separating case. In fact, by combining the definition of $\mathbf{v}$ (68) and the inequality

$$\mu \|\mathbf{v}_t\| + v_n \leqslant 0 \tag{76}$$

the non-penetration condition is recovered

$$-\dot{u}_n \leqslant 0 \tag{77}$$

In conclusion, relation (69) describes the full frictional contact law for contacting bodies. Although this relation provides further insight into such complex frictional contact laws, additional developments can still be made to establish a relationship between $-\dot{\mathbf{u}}$ and $\mathbf{r}$ based on a normality rule. To do this, the relation $\mathbf{v} \in \partial\Psi_{K_\mu}(\mathbf{r})$ needs to be further developed. We first apply the Legendre–Fenchel transform to inverse relation (69)

$$\sup_{\mathbf{r}}[\mathbf{v}\cdot\mathbf{r} - \Psi_{K_\mu}(\mathbf{r})] = \sup_{\mathbf{r}\in K_\mu}[\mathbf{v}_t\cdot\mathbf{r}_t + v_n r_n] \tag{78}$$

It is clear that the supremum will be achieved for a vector $\mathbf{r}_t$ collinear to $\mathbf{v}_t$:

$$\sup_{\mathbf{r}\in K_\mu}[\|\mathbf{v}_t\|\,\|\mathbf{r}_t\| + v_n r_n] \tag{79}$$

Taking into account that $\|\mathbf{r}_t\|$ is bounded by μr_n, we have

$$\|\mathbf{v}_t\|\,\|\mathbf{r}_t\| + v_n\, r_n \leqslant r_n(\mu\|\mathbf{v}_t\| + v_n) \tag{80}$$

Two distinct possibilities emerge: if $\mu\|\mathbf{v}_t\| + v_n \leqslant 0$ then supremum (78) is 0 since $r_n \geqslant 0$; if on the other hand $\mu\|\mathbf{v}_t\| + v_n \geqslant 0$ then since the value of r_n is unbounded, so is the supremum (78). Thus, we have

$$\sup_{r_n\in\mathbb{R}_+}[r_n(\mu\|\mathbf{v}_t\| + v_n)] = \Psi_{K_\mu^*}(\mathbf{v}) \tag{81}$$

and the inverse law is

$$\mathbf{r} \in \partial\Psi_{K_\mu^*}(\mathbf{v}) \tag{82}$$

The functions $\Psi_{K_\mu^*}(\mathbf{v})$ and $\Psi_{K_\mu}(\mathbf{r})$ satisfy the following relation:

$$\Psi_{K_\mu^*}(\mathbf{v}') + \Psi_{K_\mu}(\mathbf{r}') \geqslant \mathbf{v}'\cdot\mathbf{r}', \quad \forall\,(\mathbf{v}',\mathbf{r}') \in \mathbb{R}^3\times\mathbb{R}^3 \tag{83}$$

A pair $(\mathbf{v},\mathbf{r})$ related by the frictional contact law satisfies

$$\mathbf{v}\in\partial\Psi_{K_\mu}(\mathbf{r}) \Leftrightarrow \mathbf{r}\in\partial\Psi_{K_\mu^*}(\mathbf{v}) \Leftrightarrow \Psi_{K_\mu^*}(\mathbf{v}) + \Psi_{K_\mu}(\mathbf{r}) = \mathbf{v}\cdot\mathbf{r} \tag{84}$$

To recover a relation between the dual variables $-\dot{\mathbf{u}}$ and $\mathbf{r}$, we add $\mathbf{r}'\cdot(-\dot{\mathbf{u}}')$ to both sides of (83),

$$\forall(\mathbf{v}',\mathbf{r}')\in\mathbb{R}^3\times\mathbb{R}^3: \quad \Psi_{K_\mu^*}(\mathbf{v}') + \Psi_{K_\mu}(\mathbf{r}') + \mathbf{r}'\cdot((-\dot{\mathbf{u}}') - \mathbf{v}') \geqslant \mathbf{r}'\cdot(-\dot{\mathbf{u}}') \tag{85}$$

The left-hand side of (85) is a function of both $-\dot{\mathbf{u}}'$ and $\mathbf{r}'$, which cannot be represented as the sum of two functions, one of $-\dot{\mathbf{u}}'$ and another of $\mathbf{r}'$. We call this function a *bi-potential* and its general expression is given by

$$b_c(-\dot{\mathbf{u}}',\mathbf{r}') := \Psi_{K_\mu^*}(\mathscr{T}(-\dot{\mathbf{u}}')) + \Psi_{K_\mu}(\mathbf{r}') + \mathbf{r}'\cdot((-\dot{\mathbf{u}}') - \mathscr{T}(-\dot{\mathbf{u}}')) \tag{86}$$

By developing the right-hand side of (86) and taking into account the equivalence

$$\Psi_{K_\mu^*}(\mathscr{T}(-\dot{\mathbf{u}})) \Leftrightarrow \Psi_{\mathbb{R}_-}(-\dot{u}_n) \tag{87}$$

we obtain the bi-potential for the associated sliding rule:

$$b_c(-\dot{\mathbf{u}}, \mathbf{r}) = \Psi_{K_\mu}(\mathbf{r}) + \mu r_n \|(-\dot{\mathbf{u}}_t)\| + \Psi_{\mathbb{R}_-}(-\dot{u}_n) \tag{88}$$

The bi-potential satisfies the fundamental inequality

$$b_c(-\dot{\mathbf{u}}', \mathbf{r}') \geqslant -\dot{\mathbf{u}}' \cdot \mathbf{r}' \tag{89}$$

A strict equality is obtained in (89) for an extremal pair that is a pair $(-\dot{\mathbf{u}}, \mathbf{r})$ related by the frictional contact law:

$$b_c(-\dot{\mathbf{u}}, \mathbf{r}) = -\dot{\mathbf{u}} \cdot \mathbf{r} \tag{90}$$

Relations (89) and (90) can be combined to give

$$\forall\, \mathbf{r}' \in \mathbb{R}^3 : \quad b_c(-\dot{\mathbf{u}}, \mathbf{r}') - b_c(-\dot{\mathbf{u}}, \mathbf{r}) \geqslant -\dot{\mathbf{u}} \cdot (\mathbf{r}' - \mathbf{r}) \tag{91}$$

$$\forall -\dot{\mathbf{u}}' \in \mathbb{R}^3 : \quad b_c(-\dot{\mathbf{u}}', \mathbf{r}) - b_c(-\dot{\mathbf{u}}, \mathbf{r}) \geqslant \mathbf{r} \cdot ((-\dot{\mathbf{u}}') - (-\dot{\mathbf{u}})) \tag{92}$$

which means that

- the bi-potential is bi-convex that is $b_c(-\dot{\mathbf{u}}, \mathbf{r})$ is a convex function of $-\dot{\mathbf{u}} \in \mathbb{R}^3$ for each $\mathbf{r} \in \mathbb{R}^3$ and a convex function of $\mathbf{r} \in \mathbb{R}^3$ for each $-\dot{\mathbf{u}} \in \mathbb{R}^3$
- the flow rule and its inverse derive from the bi-potential $b_c(-\dot{\mathbf{u}}, \mathbf{r})$

$$-\dot{\mathbf{u}} \in \partial_{\mathbf{r}} b_c(-\dot{\mathbf{u}}, \mathbf{r}) \quad \text{and} \quad \mathbf{r} \in \partial_{-\dot{\mathbf{u}}} b_c(-\dot{\mathbf{u}}, \mathbf{r}) \tag{93}$$

The advantage of the present formulation results in the compact form of the law formulated with only one variational inequality. This contrast with the formulation used by Alart and Curnier where two inequalities are needed to formulated the behaviour. As it will be seen in the next sections, this writing of the frictional contact law can be advantageously exploited to derive a robust algorithm. Relations (93) are essentials for the derivation of stationary principles involving a functional that depends now on both the velocities and the stresses.

4.4. Non-associated sliding rule

To include non-associated sliding rules within the same framework, we need to modify the sliding rule as follows. It is straightforward (see Figure 6) that for r_n *fixed*, we have

$$\mathbb{Q}^2(-\dot{\mathbf{u}}_t) \in \partial \Psi_{K_\mu(r_n)}(\mathbf{r}_t) \tag{94}$$

Obviously, there is no quasi-pseudo-potential to describe such frictional model. If the sliding rule is non-associated, prior to the addition of a vector orthogonal to the tangent plane, the first step consists in applying a transformation to the tangential velocity in order to recover the normality of the slips to the friction cone in the plane $r_n = \text{const}$ (Figure 6). Next, we add the term '$-(\dot{u}_n + \|\mathbb{Q}^2(-\dot{\mathbf{u}}_t)\|_\mu^*)\mathbf{n}$' to the left-hand side of (44) to recover the normality with respect to the elliptic Coulomb's cone:

$$-(\mathbb{Q}^2\dot{\mathbf{u}}_t + (\dot{u}_n + \|\mathbb{Q}^2(-\dot{\mathbf{u}}_t)\|_\mu^*)\mathbf{n}) \in \partial \Psi_{K_\mu}(\mathbf{r}) \tag{95}$$

where K_μ is now defined by (21) and its dual by

$$K_\mu^* = \{\mathbf{v} \in \mathbb{R}^3 \mid \|\mathbf{v}_t\|_\mu^* + v_n \leqslant 0\} \tag{96}$$

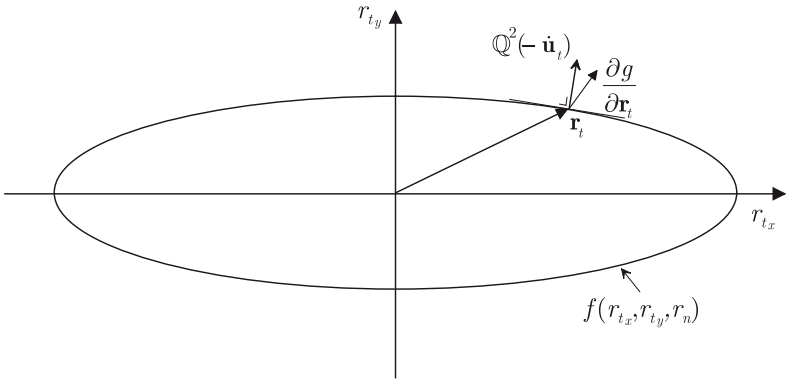

Figure 6. Non-associated sliding rule.

It is worth mentioning that the norm used in (62) cannot be arbitrary and should be chosen properly in order to ensure that the frictional contact law encompasses the case of separation. By introducing the mapping $\mathscr{T}$ defined by

$$\mathscr{T} : \mathscr{V} \mapsto \mathscr{V} : -\dot{\mathbf{u}} \mapsto -(\mathbb{Q}^2\dot{\mathbf{u}}_t + (\dot{u}_n + \|\mathbb{Q}^2(-\dot{\mathbf{u}}_t)\|_\mu^*)\mathbf{n}) \tag{97}$$

relation (69) is recovered along with its inverse, which again coincides with the indicator function of K_μ^*. Finally, we apply relation (86) with the present transformation and obtain the expression of the bi-potential (see Reference [10]):

$$b_c(-\dot{\mathbf{u}}, \mathbf{r}) = \Psi_{K_\mu}(\mathbf{r}) + \Psi_{\mathbb{R}_-}(-\dot{u}_n) + \left(\mathbb{I} - \mathbb{Q}^2\right) \cdot \mathbf{r}_t + r_n \|\mathbb{Q}^2(-\dot{\mathbf{u}}_t)\|_\mu^* \tag{98}$$

The non-associated nature of the sliding rule is characterized by an extra term that involves $-\dot{\mathbf{u}}_t$ and $\mathbf{r}_t$.

5. EVOLUTION PROBLEMS

In this section, the quasi-static isothermal evolution process occurring during frictional interaction between two elastic bodies subjected to a load history is considered. The contact force distribution response on the evolving contact area for a given displacement path over a time interval $[0, T]$ is addressed in continuous and discretized forms. The time t is conceived as a monotonically increasing arbitrary parameter, which merely orders successive events since a time-independent behaviour on the interface is assumed. In a displacement-based solution, the time-integration of the frictional-contact law is a displacement-driven process and the velocity over each time step is assumed to be constant. Here we adopt the implicit integration scheme, known in the literature as backward Euler difference, which amounts to enforcing the discrete sliding rule at the end of the step.

By transforming adequately inequality (91), the integration problem is formulated as a constrained mathematical problem where the contact reaction at the end of the time step is found as the projection of a modified augmented surface traction onto the Coulomb cone. Formulated in this way, the time-stepping algorithm encompasses naturally three possible cases: the modified augmented surface traction belongs to K_μ, to its dual K_μ^* or elsewhere. Before addressing the discretization, we recall the continuous form of the evolution problem.

5.1. Continuous form

We assume that the contact surface is known and does not change with time. This situation is encountered in the steady sliding problem, for instance. For any point on ${}^{+}\Gamma_c$, the relative velocity is governed by the implicit differential inclusion (93.a). It is observed that, for frictional interface, the velocity cannot be eliminated, which makes the stress problem and the velocity problem coupled. Locally, the evolution of the contact force $\mathbf{r}(t)$ for a given displacement path $\mathbf{u}(t)$ is a solution of the following problem

Problem $[\mathscr{P}_1]$

Find $\mathbf{r}(t)$ in $[0, T]$ such that

$\mathbf{u}(t_0) = \mathbf{u}_0,\ \mathbf{r}(t_0) = \mathbf{r}_0$

$-\dot{\mathbf{u}} \in \partial_{\mathbf{r}} b_c(-\dot{\mathbf{u}}, \mathbf{r})$ on ${}^{+}\Gamma_c$

For problems where the contact surface is known and does not change with time, the problem $[\mathscr{P}_1]$ is adequate. In a general case, the boundary ${}^{+}\Gamma_c$ changes with time and its determination within the time-interval $[0, T]$ is a part of the problem solution which can be obtained if a time-discretization is applied.

5.2. Discretized form

The time interval $[0, T]$, within which the loading history is defined, is partitioned into N sub-intervals of size $\triangle t$, not necessarily equal, according to

$$0 = t_0 < t_1 < \cdots < t_{n-1} < t_n < \cdots < t_N = T \tag{99}$$

We set $\omega(t_n) = \omega_n$ and

$$\triangle\omega_n = \omega_{n-1} - \omega_n \tag{100}$$

where ω represents any variable. The solution of the frictional contact problem within the interval $[0, T]$ is then obtained by solving N successive finite-step problems. Between two time instants, the velocity is assumed to be constant. For the sake of clarity, we focus our attention on the first time increment $[t_0, t_1]$. The problem of discrete evolution consists in evaluating variables at the end of a time step given their values at the beginning and the total displacement increment. In order to ensure convergence and stability requirements, the implicit scheme is considered. As a result of a backward-Euler type approximation, the interface law is satisfied at the end of each time step:

$$-\dot{\mathbf{u}}_1 \in \partial_{\mathbf{r}} b_c(-\dot{\mathbf{u}}_1, \mathbf{r}_1) \quad \text{on } {}^{+}\Gamma_c \tag{101}$$

Furthermore, a pair $(-\dot{\mathbf{u}}_1, \mathbf{r}_1)$ satisfying (101) is also extremal at the end of the step:

$$b_c(-\dot{\mathbf{u}}_1, \mathbf{r}_1) = -\dot{\mathbf{u}}_1 \cdot \mathbf{r}_1 \quad \text{on } {}^{+}\Gamma_c \tag{102}$$

The goal being to derive a relation between the contact force increment and the displacement increment, relations (101) and (102) are transformed such that incremental variables appear

explicitly:

$$-\triangle\mathbf{u} \in \triangle t\,\partial_{\mathbf{r}} b_c\left(-\frac{\triangle\mathbf{u}}{\triangle t}, \mathbf{r}_0 + \triangle\mathbf{r}\right) \tag{103}$$

where

$$\triangle t\,\partial_{\mathbf{r}} b_c\left(-\frac{\triangle\mathbf{u}}{\triangle t}, \mathbf{r}_0 + \triangle\mathbf{r}\right) = -\triangle\mathbf{u}\cdot(\mathbf{r}_0 + \triangle\mathbf{r}) \tag{104}$$

Taking into account that b_c positively is homogeneous of degree one in $-\dot{\mathbf{u}}$, the discretized frictional contact law turns out to be

$$-\triangle\mathbf{u} \in \partial_{\triangle\mathbf{r}}\triangle b_c(-\triangle\mathbf{u}, \triangle\mathbf{r}) \tag{105}$$

where $\triangle b_c$ is defined by

$$\triangle b_c(-\triangle\mathbf{u}, \triangle\mathbf{r}) = \triangle t\, b_c\left(-\frac{\triangle\mathbf{u}}{\triangle t}, \mathbf{r}_0 + \triangle\mathbf{r}\right) + \mathbf{r}_0\cdot\triangle\mathbf{u} \tag{106}$$

Providing that $\triangle t > 0$, this scalar-valued function is bi-convex and lower semi-continuous. Besides, it is a bi-potential since the fundamental inequality is satisfied for every arbitrary pair $(-\triangle\mathbf{u}', \triangle\mathbf{r}')$:

$$\triangle b_c(-\triangle\mathbf{u}', \triangle\mathbf{r}') \geqslant -\triangle\mathbf{u}'\cdot\triangle\mathbf{r}' \tag{107}$$

Accordingly, the inverse law is given by

$$\triangle\mathbf{r} \in \partial_{-\triangle\mathbf{u}}\triangle b_c(-\triangle\mathbf{u}, \triangle\mathbf{r}) \tag{108}$$

At this stage, it is possible to extend the discrete relations to the entire potential contact surface Γ_c. The expression of $\triangle b_c(-\triangle\mathbf{u}, \triangle\mathbf{r})$ contains the indicator function $\Psi_{\mathbb{R}_-}(-\triangle u_n)$ that enforces the impenetrability condition on ${}^{+}\Gamma_c$. By simply adding the gap $-h_0$ existing at the beginning of the time step to $-\triangle u_n$, relation (105) becomes applicable to all candidates to contact, i.e. all points on Γ_c. The indicator function related to the non-penetration condition is now $\Psi_{\mathbb{R}_+}(h_0 + \triangle u_n)$. The contact force increment $\triangle\mathbf{r}$ for a given a $\triangle\mathbf{u}$ is solution of the problem $[\mathscr{P}_2]$:

Problem $[\mathscr{P}_2]$

Find $\triangle\mathbf{r}$ such that

$-\triangle\mathbf{u} \in \partial_{\triangle\mathbf{r}}\triangle b_c(-\triangle\mathbf{u}, \triangle\mathbf{r})$ on Γ_c

The history-dependent character is clearly exhibited by the incremental form and its dependence on initial condition $\mathbf{r}_0$. Furthermore, unlike elastoplastic problems, the incremental bi-potential is not differentiable.

6. DISCRETE GOVERNING RELATIONS FOR THE FRICTIONAL CONTACT LAW WITH NON-ASSOCIATED SLIDING RULE

The differential inclusion (91) is equivalent to the following variational inequality:

$$\mathbf{r} \in \mathbb{R}^3 : \quad b_c(-\dot{\mathbf{u}}, \mathbf{r}') - b_c(-\dot{\mathbf{u}}, \mathbf{r}) \geqslant -\dot{\mathbf{u}} \cdot (\mathbf{r}' - \mathbf{r}), \quad \forall \mathbf{r}' \in \mathbb{R}^3 \tag{109}$$

which, after applying an implicit scheme, turns into

$$\mathbf{r}_1 \in \mathbb{R}^3 : \quad b_c(-\triangle\mathbf{u}, \mathbf{r}') - b_c(-\triangle\mathbf{u}, \mathbf{r}_1) \geqslant -\triangle\mathbf{u} \cdot (\mathbf{r}' - \mathbf{r}_1), \quad \forall \mathbf{r}' \in \mathbb{R}^3 \tag{110}$$

where $b_c(-\triangle\mathbf{u}, \mathbf{r}_1)$ given by

$$b_c(-\triangle\mathbf{u}, \mathbf{r}_1) = \Psi_{K_\mu}(\mathbf{r}_1) + \Psi_{\mathbb{R}_-}(-h_0 - \triangle u_n) + (\mathbb{I} - \mathbb{Q}^2)(-\triangle\mathbf{u}_t) \cdot \mathbf{r}_{t_1} + r_{n_1} \|\mathbb{Q}^2(-\triangle\mathbf{u}_t)\|_\mu^* \tag{111}$$

takes into account the gap $-h_0$ at the beginning of the time step. The variational inequality (110) is rewritten in an obvious manner as

$$\mathbf{r}_1 \in \mathbb{R}^3 : \quad \rho b_c(-\triangle\mathbf{u}, \mathbf{r}') - \rho b_c(-\triangle\mathbf{u}, \mathbf{r}_1) + [\mathbf{r}_1 - (\mathbf{r}_1 - \rho\triangle\mathbf{u})] \cdot (\mathbf{r}' - \mathbf{r}_1) \geqslant 0, \quad \forall \mathbf{r}' \in \mathbb{R}^3 \tag{112}$$

where ρ is a strictly positive number that need to be chosen in a suitable range to ensure convergence. The transformation is possible because the bi-potential is a positively homogenous function of order one with respect to $-\triangle\mathbf{u}$:

$$b_c(-\rho\,\triangle\mathbf{u}, \mathbf{r}) = \rho b_c(-\triangle\mathbf{u}, \mathbf{r}) \tag{113}$$

The variational inequality (112) means that $\mathbf{r}_1$ is the proximal point of the augmented force $\hat{\mathbf{r}} = \mathbf{r}_1 - \rho\,\triangle\mathbf{u}$, with respect to the function $\mathbf{r}_1 \mapsto \rho b_c(-\triangle\mathbf{u}, \mathbf{r}_1)$:

$$\mathbf{r}_1 = \text{prox}(\mathbf{r}_1 - \rho\triangle\mathbf{u}, \rho b_c(-\triangle\mathbf{u}, \mathbf{r}_1)) \tag{114}$$

The solution of (114) can be obtained using the Usawa's algorithm which involves two steps:

$$\text{prediction :} \quad \hat{\mathbf{r}}^{i+1} = \mathbf{r}_1^i - \rho\triangle\mathbf{u} \tag{115}$$

$$\text{correction :} \quad \mathbf{r}_1^{i+1} = \text{prox}(\hat{\mathbf{r}}^{i+1}, \rho b_c(-\triangle\mathbf{u}, \mathbf{r}_1^i)) \tag{116}$$

By substituting $b_c(-\triangle\mathbf{u}, \mathbf{r}_1)$ by its expression (111) in (112) and providing that $-h_0 - \triangle u_n \leqslant 0$, we obtain

$$\begin{aligned} &\mathbf{r}_1 \in K_\mu, \\ &\rho(\mathbb{I} - \mathbb{Q}^2)(-\triangle\mathbf{u}_t) \cdot (\mathbf{r}_t' - \mathbf{r}_{t_1}) \\ &\quad + \rho(r_n' - r_{n_1})\|\mathbb{Q}^2(-\triangle\mathbf{u}_t)\|_\mu^* [\mathbf{r}_1 - (\mathbf{r}_1 - \rho\triangle\mathbf{u})] \cdot (\mathbf{r}' - \mathbf{r}_1) \geqslant 0, \quad \forall \mathbf{r}' \in K_\mu \end{aligned} \tag{117}$$

Using the decomposition (9), the last term in (117) can be developed and the inequality rearranged to obtain:

$$\mathbf{r}_1 \in K_\mu : \quad (\mathbf{r}_{t_1} - \boldsymbol{\tau}_t) \cdot (\mathbf{r}_t' - \mathbf{r}_{t_1}) + (r_{n_1} - \tau_n)(r_n' - r_{n_1}) \geqslant 0 \quad \forall \mathbf{r}' \in K_\mu \tag{118}$$

where

$$\boldsymbol{\tau}_t = \mathbf{r}_{t_1} - \rho\mathbb{Q}^2\triangle\mathbf{u}_t \quad \text{and} \quad \tau_n = r_{n_1} - \rho(\triangle u_n + \|\mathbb{Q}^2(-\triangle\mathbf{u}_t)\|_\mu^*) \tag{119}$$

are the components of the modified augmented surface traction. The last inequality means that the reaction $\mathbf{r}$ at the end of the time step is the projection of the augmented surface traction onto the convex Coulomb's cone K_μ:

$$\mathbf{r}_1 = \text{proj}(\boldsymbol{\tau}, K_\mu) \tag{120}$$

The primary attribute of the method is that only one predictor–corrector step is required for the discrete frictional contact problem:

$$\begin{aligned} &\text{Predictor:} \quad \boldsymbol{\tau}^{i+1} = \mathbf{r}_1^i - \rho[\mathbb{Q}^2\triangle\mathbf{u}_t + (\triangle u_n + \|\mathbb{Q}^2(-\triangle\mathbf{u}_t)\|_\mu^*)\mathbf{n}] \\ &\text{Corrector:} \quad \mathbf{r}_1^{i+1} = \text{proj}(\boldsymbol{\tau}^{i+1}, K_\mu) \end{aligned}$$

In the solution of projection problem (120), three different situations must be considered according to the position of the prediction $\boldsymbol{\tau}$ in $\mathbb{R}^3$. The first case corresponds to a prediction $\boldsymbol{\tau}$ located in the cone K_μ. Its projection is the prediction itself, i.e. $\mathbf{r}_1 = \boldsymbol{\tau}$. The second one relates to a prediction situated in the cone K_μ^*, where its projection turns out to be the origin ($\mathbf{r}_1 = \mathbf{0}$). In the last case, the prediction is neither in K_μ nor in K_μ^* and the corrector step requires computing the projection of the prediction. The projection of a point onto a convex set is equivalent to the minimization of the distance between this point and the convex set:

$$\mathbf{r}_1 = \inf_{\mathbf{r}\in K_\mu} \frac{1}{2}\|\mathbf{r} - \boldsymbol{\tau}\|^2 = \inf_{\|\mathbf{r}_t\|_\mu \leqslant r_n} \frac{1}{2}[\|\mathbf{r}_t - \boldsymbol{\tau}_t\|^2 + (r_n - \tau_n)^2] \tag{121}$$

Next, problem (121) is reformulated as an unconstrained minimization problem by means of the Lagrange multipliers technique

$$\mathbf{r}_1 = \sup_{\lambda \geqslant 0} \inf_{\mathbf{r}_t, r_n} \mathscr{L}(\mathbf{r}_t, r_n, \lambda) \tag{122}$$

where

$$\mathscr{L}(\mathbf{r}_t, r_n, \lambda) = \tfrac{1}{2}[\|\mathbf{r}_t - \boldsymbol{\tau}_t\|^2 + (r_n - \tau_n)^2] + \lambda(\|\mathbf{r}_t\|_\mu - r_n) \tag{123}$$

Expressing the stationary conditions, one has

$$\frac{\partial\mathscr{L}}{\partial\lambda} = \|\mathbf{r}_{t_1}\|_\mu - r_{n_1} = 0 \tag{124}$$

$$\frac{\partial\mathscr{L}}{\partial\mathbf{r}_t} = \mathbf{r}_{t_1} - \boldsymbol{\tau}_t + \lambda\mathbb{M}^{-2}\frac{\mathbf{r}_{t_1}}{\|\mathbf{r}_{t_1}\|_\mu} = \mathbf{0} \tag{125}$$

$$\frac{\partial\mathscr{L}}{\partial r_n} = r_{n_1} - \tau_n - \lambda = 0 \tag{126}$$

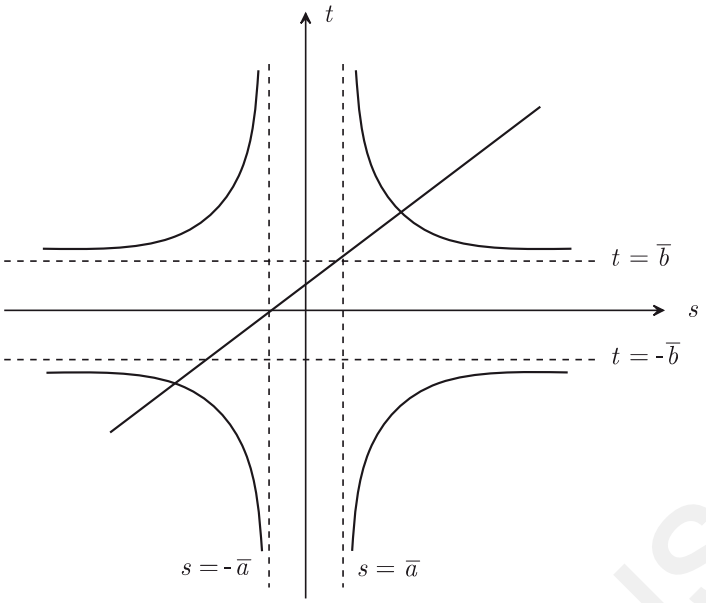

Figure 7. Geometric interpretation of the projection solution.

We combine first (124) and (126) to eliminate r_{n_1}

$$\|\mathbf{r}_{t_1}\|_\mu = \tau_n + \lambda \tag{127}$$

Next, (125) is further developed as follows:

$$r_{t_{x1}} = \|\mathbf{r}_{t_1}\|_\mu \frac{\mu_x^2\, \tau_{t_x}}{\mu_x^2\, \|\mathbf{r}_{t_1}\|_\mu + \lambda}, \quad r_{t_{y1}} = \|\mathbf{r}_{t_1}\|_\mu \frac{\mu_y^2 \tau_{t_y}}{\mu_y^2\, \|\mathbf{r}_{t_1}\|_\mu + \lambda} \tag{128}$$

By combining (127), (128) and (18), the optimization problem is reduced to finding the positive zeros of the following quartic equation:

$$\frac{\mu_x^2 (\tau_{t_x})^2}{(\mu_x^2 \tau_n + \lambda(1+\mu_x^2))^2} + \frac{\mu_y^2 (\tau_{t_y})^2}{(\mu_y^2 \tau_n + \lambda(1+\mu_y^2))^2} = 0 \tag{129}$$

Further insight into Equation (129) is gained by letting

$$\xi = 1 + \mu_x^2, \quad \eta = 1 + \mu_y^2, \quad s = \mu_x^2 \tau_n + \xi\lambda, \quad t = \mu_y^2 \tau_n + \eta\lambda, \quad \bar{a} = \mu_x^2 (\tau_{t_x})^2, \quad \bar{b} = \mu_y^2 (\tau_{t_y})^2 \tag{130}$$

so that (129) reduces to finding the intersection of a quartic and a straight line

$$\begin{aligned} &\frac{\bar{a}^2}{s^2} + \frac{\bar{b}^2}{t^2} = 1 \\ &t = \frac{\eta}{\xi}\, s + \frac{\mu_y^2 - \mu_x^2}{\xi}\, \tau_n \end{aligned} \tag{131}$$

This is illustrated graphically in Figure 7. Note that the first equation of the system has orthogonal asymptotes $s = \pm\bar{a}$ and $t = \pm\bar{b}$. Since the straight line always has positive slope,

direct inspection of the Figure 7 reveals that the system of equation has one negative root, one positive root and a pair of complex conjugate roots. For an isotropic friction condition and an associated sliding rule, an analytical solution can be obtained [7, 11]. According to the relation (120), the process is iterative and at the $(i+1)$th iteration, the local stage can be summarized by

Box 1.

Predictor:

$$\boldsymbol{\tau}^{i+1} = \mathbf{r}_1^i - \rho[\mathbb{Q}^2 \triangle \mathbf{u}_t + (\triangle u_n + \|\mathbb{Q}^2(-\triangle \mathbf{u}_t)\|_\mu^*)\mathbf{n}]$$

Corrector:

if $\|\boldsymbol{\tau}_t^{i+1}\|_\mu^* < -\tau_n^{i+1}$ *then*

$\mathbf{r}^{i+1} = \mathbf{0}$! no contact

elseif $\|\boldsymbol{\tau}_t^{i+1}\|_\mu^* \leqslant \tau_n^{i+1}$ *then*

$\mathbf{r}^{i+1} = \boldsymbol{\tau}^{i+1}$! contact with sticking

else

solve system (131) ! contact with sliding

endif

In the present approach, the algorithm does not make a distinction between the contact and the frictional problems, which are combined and solved in one single step anticipating a reduction in computing time. Furthermore, non-associated sliding rules can be accommodated without any difficulty.

7. FRICTIONAL CONTACT FINITE-STEP PROBLEM

The solution of the elastic frictional-contact initial/boundary value problem, under a given history of external actions, requires following the evolution of the body response since the frictional contact law is intrinsically path-dependant. This analysis is performed by carrying out a sub-division of the external action history $t \mapsto f^{\text{ext}}(t)$, $t \in [0, T]$, into a sequence of loading conditions at prescribed time instants so that the load path is divided into finite increments. We denote by f^{ext} the body forces and the surface tractions. The solution is then achieved by solving a sequence of problems in which the load increments are applied and the variables at the end of each increment are updated. Attention is focused on a single step of the sequence defined above that is we need to evaluate the finite increments of the unknown variables corresponding to a given increment of load when their values are assigned at the beginning of the step. For any given load increment $\triangle f^{\text{ext}}$ of the external load, the corresponding finite-step frictional-contact structural problem is governed by the following set of equations:

- in Ω_α : $\quad \text{div}\, \triangle \boldsymbol{\sigma}^\alpha + \triangle \bar{\mathbf{f}}^\alpha = \mathbf{0}$ (132)

$$\triangle \boldsymbol{\varepsilon}^\alpha = \text{grad}_s\, \triangle \mathbf{u}^\alpha \tag{133}$$

$$\triangle\boldsymbol{\sigma}^{\alpha}\cdot\triangle\boldsymbol{\varepsilon}^{\alpha}=\triangle V(\triangle\boldsymbol{\varepsilon}^{\alpha})+\triangle W(\triangle\boldsymbol{\sigma}^{\alpha}) \tag{134}$$

- on Γ_t^{α}: $\quad \mathbf{n}^{\alpha}\cdot\triangle\boldsymbol{\sigma}^{\alpha}=\triangle\bar{\mathbf{t}}^{\alpha}$ (135)
- on Γ_u^{α}: $\quad \triangle\mathbf{u}^{\alpha}=\triangle\bar{\mathbf{u}}^{\alpha}$ (136)
- on Γ_c: $\quad \triangle\mathbf{r}\in\partial_{-\triangle\mathbf{u}}\triangle b_c(-\triangle\mathbf{u},\triangle\mathbf{r})$ (137)

A displacement increment is said to be kinematically admissible (*ka*) if the compatibility conditions (133) and (136) are satisfied. A stress increment is said to be statically admissible (*sa*) if equilibrium equations (132) and (135) are satisfied. The chief advantage of following variational procedure is that the incremental force–displacement relation is obtained as a subgradient of a scalar-valued function, which open the way for the application of variational methods. By introducing the following incremental bi-functional:

$$\begin{aligned}\triangle\beta(\triangle\mathbf{u},\triangle\boldsymbol{\sigma})=&\int_{\Omega}[\triangle\mathrm{W}(\triangle\boldsymbol{\varepsilon}(\triangle\mathbf{u})+\triangle\mathrm{V}(\triangle\boldsymbol{\sigma})]\,\mathrm{d}\Omega+\int_{\Gamma_c}\triangle b_c(-\triangle\mathbf{u},\triangle\mathbf{r})\,\mathrm{d}\Gamma\\&-\int_{\Omega}\triangle\bar{\mathbf{f}}\cdot\triangle\mathbf{u}\,\mathrm{d}\Omega-\int_{\Gamma_t}\triangle\bar{\mathbf{t}}\cdot\triangle\mathbf{u}\,\mathrm{d}\Gamma-\int_{\Gamma_u}\triangle\bar{\mathbf{t}}(\triangle\boldsymbol{\sigma})\cdot\triangle\bar{\mathbf{u}}\,\mathrm{d}\Gamma\end{aligned} \tag{138}$$

finding an exact solution of the boundary value problem (132–137) over a time step is equivalent to simultaneously solving the following stationary principles:

$$\inf_{\triangle\mathbf{u}^{ka}}\triangle\beta(\triangle\mathbf{u}^{ka},\triangle\boldsymbol{\sigma}),\quad \inf_{\triangle\boldsymbol{\sigma}^{sa}}\triangle\beta(\triangle\mathbf{u},\triangle\boldsymbol{\sigma}^{sa}) \tag{139}$$

In the definition of the bi-functional, the following notations have been adopted:

$$\Omega=\bigcup_{i=1}^{\alpha}\Omega_i,\quad \Gamma_t=\bigcup_{i=1}^{\alpha}\Gamma_t^i,\quad \Gamma_u=\bigcup_{i=1}^{\alpha}\Gamma_u^i \tag{140}$$

with

$$\Gamma_t^i\bigcap\Gamma_t^j=\emptyset,\quad \Gamma_u^i\bigcap\Gamma_u^j=\emptyset,\ \ i\neq j \tag{141}$$

The minimum conditions (139) result from the convexity inequalities (91) and (92). In fact, a non-extremal pair $(\triangle\mathbf{u}^{ka},\triangle\boldsymbol{\sigma})$, will be such that

$$\triangle\beta(\triangle\mathbf{u}^{ka},\triangle\boldsymbol{\sigma})\geqslant\triangle\beta(\triangle\mathbf{u},\triangle\boldsymbol{\sigma}) \tag{142}$$

In the same way, for a non-extremal pair $(\triangle\mathbf{u},\triangle\boldsymbol{\sigma}^{sa})$, we have

$$\triangle\beta(\triangle\mathbf{u},\triangle\boldsymbol{\sigma}^{sa})\geqslant\triangle\beta(\triangle\mathbf{u},\triangle\boldsymbol{\sigma}) \tag{143}$$

It is worth mentioning that the displacement principle does not involve the last term in (138) and the stress principle does not include the fourth term. When the behaviour on the contact surface is frictionless, the bi-functional split into the sum

$$\triangle\beta(\triangle\mathbf{u},\triangle\boldsymbol{\sigma})=\triangle\Phi(\triangle\mathbf{u})+\triangle\Pi(\triangle\boldsymbol{\sigma}) \tag{144}$$

of the total energy functional

$$\triangle\Phi(\triangle\mathbf{u}) = \int_\Omega \triangle \mathrm{V}(\triangle\boldsymbol{\varepsilon}(\triangle\mathbf{u}))\,\mathrm{d}\Omega + \int_{\Gamma_c} \Psi_{\mathbb{R}_-}(-\triangle u_n)\,\mathrm{d}\Gamma - \int_\Omega \triangle\bar{\mathbf{f}}\cdot\triangle\mathbf{u}\,\mathrm{d}\Omega - \int_{\Gamma_t} \triangle\bar{\mathbf{t}}\cdot\triangle\mathbf{u}\,\mathrm{d}\Gamma \tag{145}$$

and of the total complementary energy functional

$$\triangle\Pi(\triangle\boldsymbol{\sigma}) = \int_\Omega \triangle \mathrm{W}(\triangle\boldsymbol{\sigma})\,\mathrm{d}\Omega + \int_{\Gamma_c} \Psi_{\mathbb{R}_+}(\triangle r_n)\,\mathrm{d}\Gamma - \int_{\Gamma_u} \triangle\bar{\mathbf{t}}(\triangle\boldsymbol{\sigma})\cdot\triangle\bar{\mathbf{u}}\,\mathrm{d}\Gamma \tag{146}$$

8. FINITE ELEMENT DISCRETIZATION

For numerical applications, a displacement formulation of the finite element method is used. The displacement and strain increment fields are approximated according to:

$$\triangle\mathbf{u}(\mathbf{X}) = \mathbf{N}(\mathbf{X})\triangle\mathbf{U}, \quad \triangle\boldsymbol{\varepsilon}(\mathbf{X}) = \mathbf{B}(\mathbf{X})\triangle\mathbf{U}, \quad \mathbf{B}(\mathbf{X}) = \mathrm{grad}_s\mathbf{N}(\mathbf{X}) \tag{147}$$

where $\triangle\mathbf{U}$ is the unknown nodal displacement increment vector and $\mathbf{N}(\mathbf{X})$ is a matrix of polynomial shape functions. The compatibility conditions (136) on Γ_u are enforced by substituting nodal unknowns on Γ_u by their corresponding values. Introducing the generalized nodal force increment vector

$$\triangle\mathbf{F}^{\mathrm{ext}} = \int_\Omega \mathbf{N}^{\mathrm{T}}\triangle\bar{\mathbf{f}}\,\mathrm{d}\Omega + \int_{\Gamma_t} \mathbf{N}^{\mathrm{T}}\triangle\bar{\mathbf{t}}\,\mathrm{d}\Gamma \tag{148}$$

the discretized form of the bi-functional (138) becomes

$$\triangle\beta(\triangle\mathbf{U}, \triangle\boldsymbol{\sigma}) = \int_\Omega [\triangle W(\triangle\boldsymbol{\varepsilon}(\triangle\mathbf{U}) + \triangle V(\triangle\boldsymbol{\sigma})]\,\mathrm{d}\Omega + \int_{\Gamma_c} \triangle b_c(-\triangle\mathbf{U}, \triangle\mathbf{R})\,\mathrm{d}\Gamma - \triangle\mathbf{F}^{\mathrm{ext}}\cdot\triangle\mathbf{U}$$

Combining the structural equilibrium equations resulting from the minimum condition (139.a) with incremental laws in Ω and on Γ_c, the solution of the boundary value problem over a time step is obtained by solving the following system of equations:

- $$\int_\Omega \mathbf{B}^{\mathrm{T}}\triangle\boldsymbol{\sigma}\,\mathrm{d}\Omega - \triangle\mathbf{F}^{\mathrm{ext}} - \triangle\mathbf{R} = \mathbf{0} \tag{149}$$
- $$\triangle\boldsymbol{\sigma} = \frac{\partial\triangle \mathrm{V}(\mathbf{B}\triangle\mathbf{U})}{\partial\triangle\boldsymbol{\varepsilon}} \tag{150}$$
- $$\triangle\mathbf{R} \in \partial_{-\triangle\mathbf{U}}\triangle b_c(-\triangle\mathbf{U}, \triangle\mathbf{R}) \quad \text{on } \Gamma_c \tag{151}$$
- $$\triangle\mathbf{U} = \triangle\bar{\mathbf{U}} \quad \text{on } \Gamma_u \tag{152}$$

where $\triangle\mathbf{R}$ are nodal contact force consistent with $\triangle\mathbf{U}$. To solve the equations system (149)–(152), an iterative method is used. For each iteration, two stages are

accomplished:

- a global stage during which $\triangle\boldsymbol{\sigma}$ and $\triangle\mathbf{R}$ are fixed and a new approximation of $\triangle\mathbf{U}$ is obtained using only one Newton's iteration which involves the computation of the stiffness matrix,
- a local stage for which $\triangle\mathbf{U}$ is fixed and new approximations of $\triangle\boldsymbol{\sigma}$ and $\triangle\mathbf{R}$ are computed according to relations (150) and (151).

9. NUMERICAL APPLICATION: COMPRESSION OF A CYLINDER IN CONTACT WITH A RIGID PLATE

In previous papers [7, 11], several applications involving frictional contact problems with isotropic friction condition and associated sliding rule have been carried out using an algorithm based on the bi-potential approach. The examples treated have shown that the algorithm is very competitive as the augmentation phase involves only one prediction–correction step. We propose, in this paper, a benchmark test to validate the algorithm for a class of non-associated anisotropic friction laws. The test of such frictional contact laws requires a 3D finite element model. The problem under consideration is a deformable elastic cylinder in contact with a rigid surface (Figure 8). The radius and the height of the cylinder are both equal to 10 mm. The Young modulus E of the cylinder is taken equal to 210 000 MPa and the Poisson ratio is 0.3. On the contact surface, the friction condition is assumed to be anisotropic. A vertical rigid motion is imposed on the upper surface of the cylinder by an amount of 0.1 mm. The displacement is applied in one step. The base of the cylinder is in contact with the rigid plate whose normal vector is $(0, 0, 1)$. The cylinder is subdivided into 1280 eight-node brick-like elements as shown in Figure 8. Each element has 27 integration points. The analysis is performed on a PC (Pentium III 733 MHz). Five different sets of frictional parameters, shown in Table I, are considered. The first case corresponds to a classical isotropic friction condition, considered here for comparison with anisotropic cases. Cases 2 and 3 represent an anisotropic frictional model with an associated sliding rule. The anisotropy is mild in case 2. The last two cases consider a non-associated sliding rule.

Figure 9 shows the contour plots of the slip and the relative displacements between the lower surface of the cylinder and the rigid plate in the x-direction. The slip correspond to the Euclidean norm of the tangential displacement. The frictional model being isotropic,

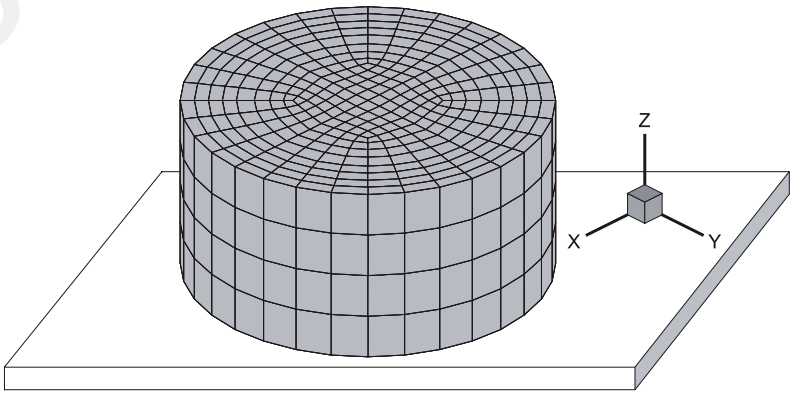

Figure 8. Compression of a cylinder in contact with a rigid plate.

Table I. Frictional properties.

Case	μ_x	μ_y	p_x	p_y
1	0.20	0.20	0.20	0.20
2	0.30	0.25	0.30	0.25
3	0.30	0.15	0.30	0.15
4	0.30	0.15	0.20	0.20
5	0.30	0.15	0.05	0.20

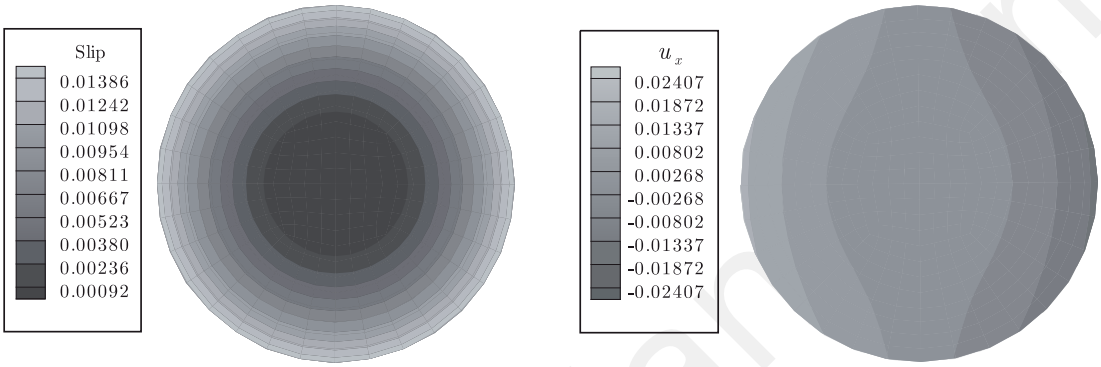

Figure 9. Case 1: (a) contour plot of slip; and (b) contour plot of u_{t_x}.

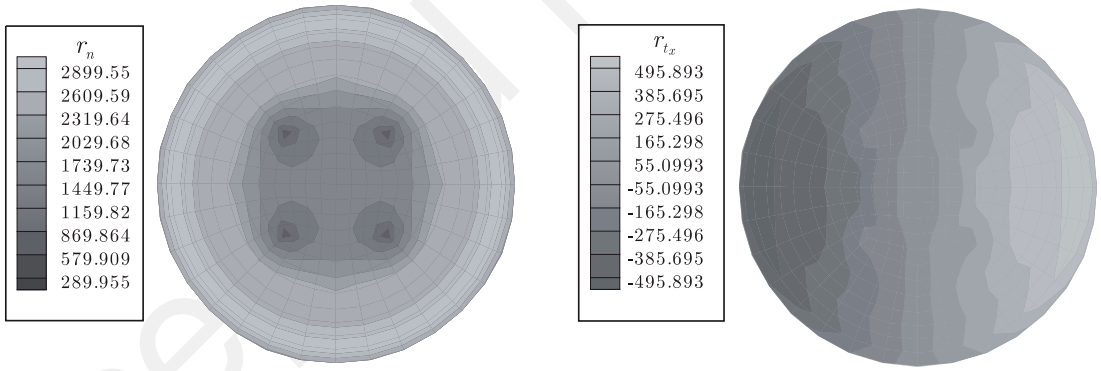

Figure 10. Case 1: (a) contour plot of r_n; and (b) contour plot of r_{t_x}.

the iso-values of the slips are circular. As expected, the stick zone is located around the base centre and sliding increases monotonically as we get closer the periphery. The magnitude of the tangential displacement in the x-direction is the largest on the cylinder edge. Figure 10 shows, for case 1, the iso-values of the normal component of the contact reaction and the tangential component of the contact reaction in the x-direction. In all figures, the x-axis is horizontal and the y-axis is vertical. Since the model is isotropic, a simple rotation about the z-axis of 90^0 gives the tangential component of the contact reaction in the y-direction. The normal reaction is higher in the periphery of the cylinder and decreases as we approach the center of the cylinder basis. However, the decrease is not monotonic along every radius. Indeed, the normal reaction

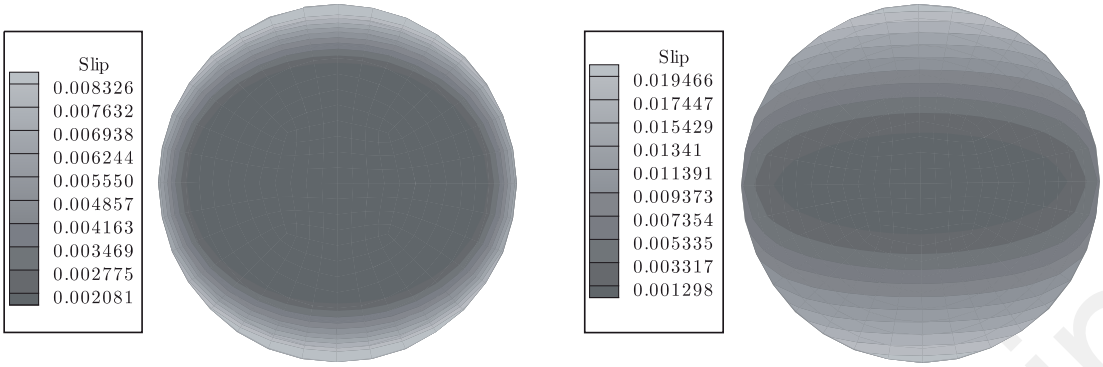

Figure 11. Contour plots of slip: (a) case 2; and (b) case 3

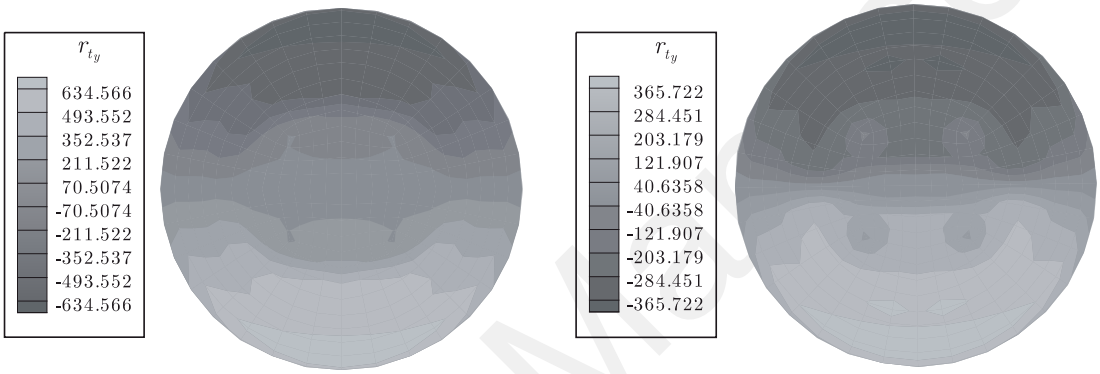

Figure 12. Contour plots of r_{t_x}: (a) case 2; and (b) case 3.

attains its minimum in four tiny areas located at approximately the third of the radius from the base centre. For all cases considered, contour plots of the normal component of the contact reaction have similar pattern. The tangential reaction is higher in the periphery of the cylinder as sliding is more important there. Now, the effect of anisotropy is considered. Slip contour plots for cases 2 and 3 are shown Figure 11. As it can be seen, the anisotropy of the friction condition influences significantly the slip distribution pattern. The stick area is now an ellipse with a semi-axes ratio equal to the semi-axes ratio of the friction criterion. The slips increases gradually from the stick area and are maximum on the periphery in the y-direction since for both cases μ_x is greater then μ_y. If the disparity between the friction coefficients μ_x and μ_y is significant (as it is for case 3) the distribution of r_{t_y} changes notably, but the iso-values pattern of r_{t_x} remains similar to the isotropic case 1 (see Figure 12). The algorithm is still convergent if the sliding rule is non-associated but requires a few more iteration. The number of iterations depends strongly on the degree of non-associativity. A ratio μ_x/μ_y much larger or much smaller than the ratio p_x/p_y gives a strong non-associated sliding rule. In Case 4, an isotropic sliding potential is considered which corresponds here to a mild non-associativity. In practice, high non-associativity (case 5) is often observed [2, 12]. Once a non-associative sliding rule is considered, the slip distribution can change drastically according to the degree of non-associativity. Indeed, if the slip rule is strongly non-associated, the iso-values of the slip become non-convex as shown Figure 13. With an isotropic sliding potential, the stick zone

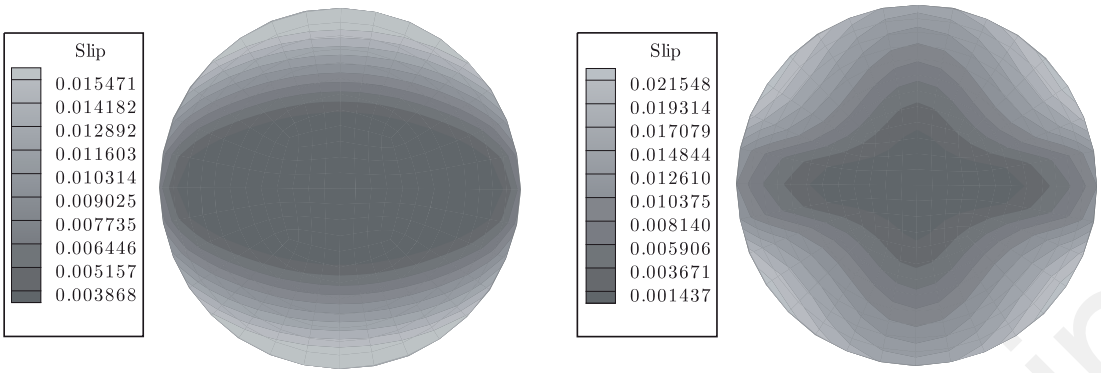

Figure 13. Contour plots of slip: (a) case 4; and (b) case 5.

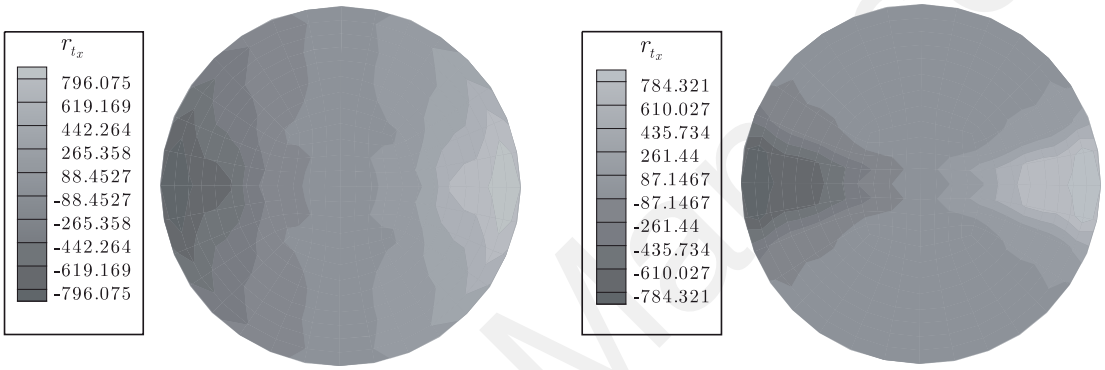

Figure 14. Contour plots of r_{t_x}: (a) case 4; and (b) case 5.

is elliptical and the maximum displacement is lower than the one obtained with an associated sliding rule. Although, the principal friction coefficients are the same for both cases 4 and 5, the maximum slip is larger for case 5. The distribution pattern of r_{t_y} (Figure 14) is similar to cases 2 and 3 (see Figure 11(a)) but the iso-values distribution of r_{t_x} is totally different if the non-associativity is strong.

10. CONCLUSIONS

In this paper, an algorithm for solving the frictional contact problem with a non-associated sliding rule has been presented. This algorithm is based on a variational formulation of the frictional contact law described by an anisotropic friction condition and a non-associated sliding rule. The frictional contact law and its inverse are obtained by applying the normality rule to a single scalar-valued function called a bi-potential. Exploiting the variational structure of the frictional contact law, the time-integration of the frictional contact law takes the form of a projection onto a convex set and only one predictor–corrector step is needed to address all cases (sticking, sliding, no-contact). The convexity properties of the bi-potential permit to associate stationary principles with initial/boundary value problems. A robust algorithm, developed by de Saxcé and Feng [3, 7] for the frictional contact law with associated sliding rule, has been

adapted to handle non-associated sliding rules. This algorithm has been successfully tested on an example.

REFERENCES

1. Wriggers P. *Computational Contact Mechanics*. Wiley: New York, 2002.
2. Michałowski R, Mróz Z. Associated and non-associated sliding rules in contact friction problems. *Archives of Mechanics* 1978; **30**(11):259–276.
3. Halphen B, Nguyen Quoc Son. Sur les matériaux standard généralisés. *Journal de Mécanique* 1975; **14**: 39–63.
4. Nguyen Quoc Son. Matériaux élasto-visco-plastique et élastoplastique à potentiel généralisé. *Comptes Rendus de l'Académie des Sciences* 1973; **277**:915–918.
5. Nguyen Quoc Son. On the elastic plastic initial-boundary value problem and its integration. *International Journal for Numerical Methods in Engineering* 1977; **11**:817–832.
6. Alart P, Curnier A. A mixed formulation for frictional contact problems prone to Newton-like solution methods. *Computer Methods in Applied Mechanics and Engineering* 1991; **92**:353–375.
7. de Saxcé G, Feng ZQ. New inequality and functional for contact friction: the implicit standard material approach. *Mechanics of Structures and Machines* 1991; **19**:301–325.
8. Hjiaj M. *Sur la Classe des Matériaux Standard Implicites*: *Concept*, *Aspects discréisés et Estimation de l'erreur a posteriori*. PhD Thesis (in French) 1999, Polytechnic Faculty of Mons, Belgium.
9. Hjiaj M, Bodovillé G, de Saxcé G. Matériaux viscoplastiques et lois de normalité implicites. *Comptes Rendus de l'Académie des Sciences Séries* IIB Mechanics 2000, **328**(9):519–524.
10. Hjiaj M, de Saxcé G, Mróz Z. A variational-inequality based formulation of the frictional contact law with a non-associated sliding rule. *European Journal of Mechanics – A/Solids* 2002; **21**:49–59.
11. de Saxcé G, Feng ZQ. The bi-potential method: a constructive approach to design the complete contact law with friction and improved numerical algorithms. *Mathematical and Computer Modelling* 1998; **28**(6): 225–245.
12. Mróz Z, Stupkiewicz S. An anisotropic friction and wear model. *International Journal of Solids and Structures* 1994; **31**:1113–1131.
13. Moreau JJ. La notion de sur-potentiel et les liaisons en élastostatique. *Comptes Rendus de l'Académie des Sciences* 1968; **267**:954–957.
14. Moreau JJ. Sur les lois de frottement, de plasticité et de viscosité. *Comptes Rendus de l'Académie des Sciences* 1970; **271**:608–611.
15. Rockafellar RT, Wets J-B. *Variational Analysis*. Springer: Berlin, 1998.
16. He Q-C, Curnier A. Anisotropic dry friction between two orthotropic surfaces undergoing large displacements. *European Journal of Mechanics – A/Solids* 1993; **12**:631–666.
17. Mróz Z. *Mathematical Models of Inelastic Behaviour*.
18. Christensen PW, Klarbring A, Pang JS, Strömberg N. Formulation and comparison of algorithms for frictional contact problems. *International Journal for Numerical Methods in Engineering* 1998; **42**:145–173.
19. Nguyen Quoc Son. *Contribution l'étude macroscopique de l'élastoplasticité avec écrouissage*. University of Waterloo Press: Canada, 1973.